

Characterisation of the dynamics of past droughts

Diaz, Vitali; Corzo Perez, Gerald A.; Van Lanen, Henny A.J.; Solomatine, Dimitri; Varouchakis, Emmanouil

DOI

10.1016/j.scitotenv.2019.134588

Publication date 2020

Document Version Final published version

Published in Science of the Total Environment

Citation (APA)

Diaz, V., Corzo Perez, G. A., Van Lanen, H. A. J., Solomatine, D., & Varouchakis, E. A. (2020). Characterisation of the dynamics of past droughts. Science of the Total Environment, 718, Article 134588. https://doi.org/10.1016/j.scitotenv.2019.134588

Important note

To cite this publication, please use the final published version (if applicable). Please check the document version above.

Other than for strictly personal use, it is not permitted to download, forward or distribute the text or part of it, without the consent of the author(s) and/or copyright holder(s), unless the work is under an open content license such as Creative Commons.

Takedown policy
Please contact us and provide details if you believe this document breaches copyrights. We will remove access to the work immediately and investigate your claim.

Green Open Access added to TU Delft Institutional Repository 'You share, we take care!' - Taverne project

https://www.openaccess.nl/en/you-share-we-take-care

Otherwise as indicated in the copyright section: the publisher is the copyright holder of this work and the author uses the Dutch legislation to make this work public.

FISEVIER

Contents lists available at ScienceDirect

Science of the Total Environment

journal homepage: www.elsevier.com/locate/scitotenv



Characterisation of the dynamics of past droughts



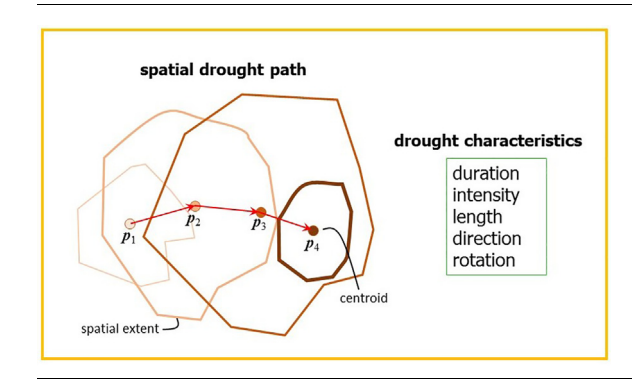
Vitali Diaz ^{a,b,*}, Gerald A. Corzo Perez ^a, Henny A.J. Van Lanen ^c, Dimitri Solomatine ^{a,b,d}, Emmanouil A. Varouchakis ^e

- ^a IHE Delft Institute for Water Education, Hydroinformatics Chair group, Delft, 2601 DA, the Netherlands
- ^b Delft University of Technology, Water Resources Section, Delft, the Netherlands
- ^c Hydrology and Quantitative Water Management Group, Wageningen University, Wageningen, the Netherlands
- ^d Water Problems Institute of the Russian Academy of Sciences, Moscow, Russia
- ^e School of Environmental Engineering, Technical University of Crete, Chania, Greece

HIGHLIGHTS

- An analysis on the characterisation of drought dynamics is presented.
- Location, spatial paths, direction, and rotation of droughts were calculated.
- Spatial patterns of the most severe droughts were analysed.
- Calculated droughts were compared with documented information.

G R A P H I C A L A B S T R A C T



ARTICLE INFO

Article history:
Received 17 March 2019
Received in revised form 9 August 2019
Accepted 19 September 2019
Available online 18 November 2019

Editor: Ralf Ludwig

Keywords: Spatio-temporal drought analysis Drought tracking Drought dynamics Drought characterisation

ABSTRACT

Drought is a complex natural phenomenon. The description of the way in which drought changes (moves) in space may help to acquire knowledge on its drivers and processes to improve its monitoring and prediction. This research presents the application of an approach to characterise the dynamics of drought. Tracks, severity, duration, as well as localisation (onset and end position), and rotation of droughts were calculated. Results of calculated droughts were compared with documented information. Data from the Standardized Precipitation Evaporation Index (SPEI) Global Drought Monitor was used to identify droughts in India as an example for the period 1901–2013. Results show regions where droughts with considerable coverage tend to occur. Paths, i.e. consecutive spatial tracks, of six of the most severe reported droughts were analysed. In all of them, areas overlap considerably over time, which suggest that drought remains in the same region for a period of time. Results of this research are being used to build a model to predict the spatial drought tracks, incl. India (https://www.researchgate.net/project/STAND-Spatio-Temporal-ANalysis-of-Drought).

© 2019 Elsevier B.V. All rights reserved.

1. Introduction

Drought has caused numerous and extensive damage around the world (Below et al., 2007; Sheffield and Wood, 2011; Tallaksen and Van Lanen, 2004; Wilhite, 2000). It has been observed across the world (Van Lanen et al., 2013). Its frequency

^{*} Corresponding author.

E-mail addresses: vdiazmercado@tudelft.nl, vitalidime@gmail.com (V. Diaz).

varies from one region to another (Andreadis et al., 2005; Sheffield et al., 2009; Tallaksen et al., 2009).

Although there is no unique definition of drought, it is generally described as a result of precipitation and temperature anomalies in a given region (Mishra and Singh, 2010; Van Loon, 2015). The spatial dimension of drought has been study in last decades in order to improve its monitoring and description (Andreadis et al., 2005; Corzo Perez et al., 2011; Diaz et al., 2018; Diaz et al., 2019; Herrera-Estrada et al., 2017; Lloyd-Hughes, 2012; Sheffield et al., 2009; Tallaksen et al., 2009; Van Loon, 2015). It has been highlighted that a better understanding of the spatial characteristics of drought (e.g. spatial extent, location) may improve the way in which it is monitored and thereby reduce its impacts.

One of the first studies in which the spatial extent (area) of drought is taken into account is the work of Yevjevich (1967). He considers drought as a phenomenon with a territorial extension. In his work, the time series of drought areas is calculated with precipitation data. The time series of drought areas is also used to define the onset, end, and duration of each drought. In the absence of observed precipitation, it was foreseen the application of the methodology with the help of synthetic data. After, Yevjevich and Karplus (1973) based on the methodology of Yevjevich (1967) present an application with precipitation data in two regions of the United States. The spatial extent is calculated through the use of Thiessen polygons. They propose the use of a grid system for the representation and handling of data, but it is not implemented. In a grid system, information is arranged in a matrix of columns and rows, where each cell has a geographical location. In each time step, the information represented in each cell can change.

Following the work of Yevjevich and Karplus (1973), Tase (1976) calculates drought areas with information arranged in a grid system, i.e. grid data. Due to the limited availability of stations records, a technique based on Monte Carlo simulation is applied for the generation of synthetic information. An application where drought areas are computed with grid data, which was interpolated from stations, is the study of Bhalme et al. (1980). They conduct a drought analysis on a monthly basis for India using precipitation. Droughts were categorised from the most severe (the largest average area) and in this way, the worst years in drought were found. In Europe, Zaidman et al. (2002) estimate the drought area with rainfall and runoff information. The data were spatially interpolated from stations. They obtained time series of drought areas that were used to calculate the onset, end and duration, among others.

The aforementioned investigations consider the entire drought area of the region under analysis as the spatial extent of the phenomenon. However, Andreadis et al. (2005) propose a methodology where the area is not considered as a whole, but as a contiguous portion defined in space and time. Through a clustering technique applied to the grid data, they calculate what are called drought events. Each calculated drought event has a duration and an area. After, Corzo Perez et al. (2011) introduce a methodology similar to that of Andreadis et al. (2005) where the centroid of the cluster is proposed to define the geographic location of the drought. The methodology is applied in global simulated runoff data. On the other hand, with a technique based on Andreadis et al. (2005), Lloyd-Hughes (2012) calculates drought events in Europe with precipitation. Each drought event is defined in three dimensions. In this study, each drought has a duration, a location, and a volume (number of cells in drought).

Posteriorly, Herrera-Estrada et al. (2017) present an analysis of how drought moves in space. The spatial tracking of droughts is performed by calculating the displacement between consecutive areas in time. In this way, they identified the tracks. On the other hand, Diaz et al. (2018) present a methodology to build the spatial

path of a drought. A path is defined as successive spatial tracks of drought. They propose the calculation of such a path to define the onset and end of each drought in time and in space. They foresee that the information provided by the calculation of these drought paths can be used to build a model that helps to predict the drought, particularly its location and spatial extent.

Drought characterisation, i.e. the calculation of its severity, duration, spatial extent, location, among others, has been improving in light of the new data availability and advances in spatiotemporal analysis. This research aims to present the application of an approach to describe the way in which drought changes (moves) in space, namely drought dynamics. This study is a continuation of the work of Diaz et al. (2019, 2018). Each drought is defined by an onset and an end in time and in space. The severity, duration, as well as the length of paths, localisation (onset and end position), and rotation of droughts were calculated. To illustrate the calculation procedure, data from the Standardized Precipitation Evaporation Index (SPEI) Global Drought Monitor (Beguería et al., 2014) was used to identify droughts in India for the period 1901–2013. Results of calculated droughts were compared with documented information.

2. Methods and data

2.1. Characterisation of drought dynamics

In this study, drought is defined in space and time. This definition relies on tracking the spatial extent (area) of the drought in each time step. A general approach to calculate the drought area is described as follows (Corzo Perez et al., 2011; Diaz et al., 2019). From hydro-meteorological data arranged in a grid system, the water anomaly is calculated in each cell in each time step with the help of a drought indicator (Mishra and Singh, 2010; Wanders et al. (2010)). A drought indicator is a mathematical formulation that converts the hydro-meteorological information into values that indicate the water anomalies. The drought indicator retains the same configuration of the grid system.

After the calculation of the drought indicator (DI), the condition of drought is indicated in each cell of the grid system. When the DI is below a threshold T, the value of 1 is placed in the cell to indicate that it is in drought; otherwise, the value of 0 is used (Eq. (1)). This binary representation of the drought state (D_s), i.e. drought or nondrought, is performed with the Eq. (1), which is applied in each cell in each time step (t).

$$D_{S}(t) = \begin{cases} 1 & \text{if } DI(t) \le T \\ 0 & \text{if } DI(t) > T \end{cases}$$
 (1)

For a given region, the drought area (DA) at the time step t can be calculated in percentage as the ratio between the number of cells in drought and the total number of cells in the region (N) (Eq. (2)). The cell number is denoted by c.

$$DA(t) = 100/N \cdot \sum_{c=1}^{N} D_{S}(t)$$
 (2)

Once the binary representation of the drought condition is concluded, the drought is characterised. This characterisation involves two phases: (1) drought paths calculation, and (2) drought characteristics calculation. In the following sections, both phases are described. Fig. 1 shows a schematic overview of the methodology carried out in this research.

2.1.1. Phase 1. Drought paths calculation

The first phase encompasses the calculation of the spatial drought paths. A spatial drought path is defined as the union of consecutive tracks in time. These drought tracks provide informa-

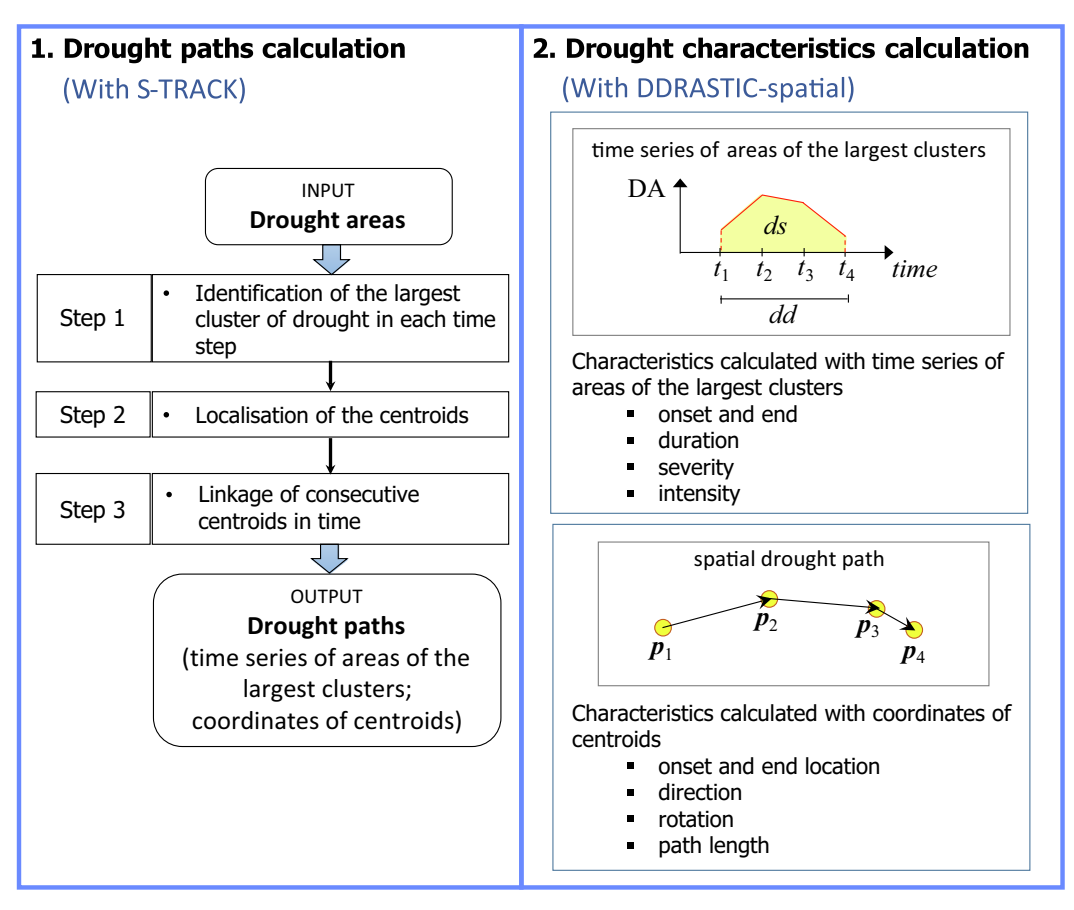


Fig. 1. Schematic overview of the methodology for the characterisation of drought dynamics that involves two phases: (1) drought paths calculation (left), and (2) drought characteristics calculation (right). In the spatial drought path scheme (right), centroid (p) is indicated by a point. The subscript indicates the time step. Arrows point out the direction of each drought track. DA, ds, and dd stand for drought area, severity, and duration, respectively.

tion on how drought moves spatially along the time. Every drought path has an onset and an end in time and in space. We followed the algorithm for spatial drought tracking called S-TRACK method presented by Diaz et al. (2018). The main assumption of S-TRACK is that drought can be monitored in space by following the location of the centroid of its spatial extent (area). The tracking algorithm consists of three steps: (1) identification of the largest cluster of drought in each time step; (2) localisation of the centroids; and (3) linkage of consecutive centroids in time (Fig. 1 (left)). The three steps of S-TRACK algorithm are described as follows.

Step 1. Identification of the largest cluster of drought

For the calculation of drought paths, the data from the binary representation of the drought state is used. As mentioned, in this data, the state of drought and non-drought is indicated with 1 s and 0 s, respectively, in each cell in each time step. The first task to identify the largest cluster of drought in each time step is the calculation of contiguous drought areas (CDA). By means of a connected-component labelling approach, the clustering of CDAs is performed. This approach connects neighbouring cells in drought (cells with a value of 1) (Corzo Perez et al., 2011). This procedure allows the calculation of the largest cluster (the one with the maximum area) in each time step.

Step 2. Localisation of the centroids

The centroid (p) is calculated for the largest cluster in each time step (Fig. 1). Coordinates of this point are used to define the geographic location of each drought area.

Step 3. Linkage of consecutive centroids in time

Two consecutive centroids in time are linked (or not) through the application of an algorithm that takes into account both the cluster area (A) and the distance between the centroids (Δl). These two variables $(A \& \Delta l)$ are limited with the use of four threshold parameters denoted by a, b, c, and d. The first two control A and the last two control Δl . The linkage of consecutive centroids in time is performed as follows. Firstly, the cluster area A is located in one of the two area size categories: normal or very large. A cluster has a normal size if A is above the parameter a and below the parameter b. If A is above the parameter b, the cluster has a very large size. When A is below the parameter a, the centroid of the cluster is not connected, and the procedure ends. After the categorisation of the cluster area, the distance between centroids Δl is analysed. For a normal size area, if Δl is below the parameter c, the centroid is linked. On the other hand, in the case of a very large size area, the centroid is linked if Δl is below the parameter d. The distinction between two area sizes was proposed due to it may happen that in very large areas the centroids can be located very far from each other, and then the distance between them fall outside of the limit established by a single parameter of distance. For this reason, two parameters are used to constrain Δl . The union of two centroids is called drought track.

After the application of S-TRACK method, two main outputs are obtained for each drought path: the coordinates of the centroids (x, y), and the areas of the largest clusters (DAs) (Fig. 1 (right)). The procedure for the calculation of drought characteristics is described in the following paragraph.

2.1.2. Phase 2. Drought characteristics calculation

After the calculation of drought paths, the onset and end in time, duration, severity, as well as the onset and end location, length of the path, and rotation are calculated for each drought

(Fig. 1 (right)). It is considered that a drought has an onset and an end in time and in space in the same way as Andreadis et al. (2005), Corzo Perez et al. (2011), Herrera-Estrada et al. (2017), and Lloyd-Hughes (2012). We follow the DDRASTIC-spatial methodology to calculate the aforementioned characteristics. DDRASTIC-spatial stands for Drought DuRAtion, SeveriTy and Intensity Computing-spatial events. This methodology is based on the work of Diaz et al. (2019). In this approach, severity is related to the temporal change of the size of the drought area (DA). In this second phase, two outputs of the drought paths calculation phase are used: time series of areas of the largest clusters, and coordinates of centroids. Phase 2 is organised in two steps according to the characteristics calculated with each type of output obtained in phase 1.

Step 1. Characteristics calculated with time series of areas of the largest clusters

Drought duration (dd) and severity (ds) are obtained with Eqs. (3) and (4), respectively (Fig. 1 (right)). The times ti and tf are the onset and end of the drought. DA is the drought area at each time step t (Eq. (2)). Drought intensity (di) is expressed as the ratio between duration and severity (Eq. (5)). Drought areas correspond to those of the largest clusters.

$$dd = ti - tf + 1 \tag{3}$$

$$ds = \sum_{t=t}^{tf} DA(t) \tag{4}$$

$$di = ds/dd (5$$

Step 2. Characteristics calculated with coordinates of centroids With the centroids of the first and last cluster, the onset and end location are identified. The position (location) of a centroid can be one of the following: centre (C), east (E), northeast (NE), north (N), northwest (NW), west (W), southwest (SW), south (S) and southeast (SE). Arbitrarily, the origin of the axes to define the location is located in the centroid of the region under study. Direction is defined with the onset and end location.

Rotation (dr) is determined with the coordinates x and y of the n centroids of each drought path (Eq. (6)). To define rotation, two labels are proposed: mostly clockwise (mc), and mostly counter-clockwise (mcc). Eq. (6) is based on the methodology for the calculation of a polygon area where coordinates of its vertices are used. In that methodology, the area is calculated as half the absolute value of ρ . When ρ is below zero, rotation is assigned as mostly clockwise; when ρ is above zero, rotation is mostly counter-clockwise; and when ρ is zero, rotation is not defined.

$$\rho = (x_1 - x_n)(y_1 + y_n) + \sum_{i=1}^{n-1} (x_{i+1} - x_i)(y_{i+1} + y_i)$$
 (6)

Finally, the length of each drought path (L) is calculated as the sum of the lengths of all the sections (drought tracks).

2.2. Study area and data

To illustrate the procedure to apply the approach to characterise the dynamics of droughts, we have selected a "real-world case", i.e. India, which regularly suffers from drought. In principle, any other region would also qualify. Moreover, we have selected the Standardized Precipitation Evaporation Index (SPEI) (Vicente-Serrano et al., 2010), but any other drought indicator can be chosen. Data from the SPEI Global Drought Monitor (http://spei.csic.es/) was used (Beguería et al., 2014) for drought tracking and characterisation of drought dynamics. SPEI has been extensively tested in many studies (Bachmair et al., 2015, 2016; Blauhut et al., 2016;

Stagge et al., 2015; Vicente-Serrano et al., 2012; Xu et al., 2015). Methodology to calculate SPEI is similar to that used in the Standardized Precipitation Index (SPI) proposed by Mckee et al. (1993), but considering the difference between precipitation (P) and potential evaporation (E) instead of only P. SPEI data from the drought monitor are in a grid form for different temporal aggregation periods. In this study, we used SPEI-6, which corresponds to anomalies of the six-month accumulation of P - E. This aggregation usually refers to extended periods of lack of water availability; therefore consequences of what is commonly called meteorological drought are closer to that caused by the so-called hydrological drought (World Meteorologic Organization (WMO). (2012)). In this study, we consider arbitrarily SPEI-6 as the drought indicator to characterise past droughts. The analysis was conducted on a monthly basis. The spatial resolution of SPEI-6 data is 0.5 degree.

2.3. Experimental setup

2.3.1. Drought areas calculation

The drought tracking algorithm focuses on the analysis of the largest drought areas, which can represent the most severe droughts. As mentioned in the description of S-TRACK (Sect. 2.1.1), within the algorithm, a clustering technique is performed in each time step to calculate the largest cluster of all cells in drought. Before the application of S-TRACK, we checked the similarity in size of the entire area in drought and that of the largest cluster.

This first task can be considered as an evaluation of the suitability of the application of S-TRACK method. The main objective is to verify that the area of the largest cluster is very close to the total. If not, when more than one spatial extent is present at the same time step, the current version of S-TRACK may miscalculate the path. The modification of S-TRACK algorithm is beyond the scope of this work.

Drought areas were calculated for the period 1901-2013 on a monthly basis. The drought indicator threshold (T) of -1 was used to indicate drought in each cell of the SPEI-6 data with Eq. (1). This approach allowed the computation of the area in percentage as the ratio between the number of cells in drought and the total number of cells in the region (1,173 cells in total in India). The entire area in drought (DA) was computed in each time step considering all cells in drought with Eq. (2). For the case of that of the largest cluster (DA_largest), firstly, the same clustering technique used by S-TRACK method was carried out to calculate the largest clusters and then the areas were computed following the procedure applied in DA.

2.3.2. Parameters selection for the spatial tracking algorithm

In S-TRACK method, four thresholds parameters have to be set: a, b, c and d. Parameter c is used as the threshold of the distance between centroids to join areas between the interval indicated by parameters a and b. On the other hand, parameter d is used to connect areas above the threshold indicated by the parameter b. The most suitable parameters are those that allow the identification of well-known droughts that occurred in the study region. In this research, two sources that present relevant information from reported droughts were retrieved and analysed as an example. These are the Emergency Events Database (EM-DAT) (Guha-Sapir, 2018) and the work of Bhalme et al. (1980), here denoted as EMD and B&M, respectively.

A catalogue of reported droughts was elaborated for the period 1901 to 2013 based on the analysis of the works of EMD and B&M. Table A1 (Appendix A) presents a summary of the information reported by EMD and B&M on the reported droughts (columns 2 to 5). The droughts are indicated per year, as presented in EMD

and B&M (column 2). EMD provides an identifier (Id) for each drought (column 3). In 1964, EMD points out two droughts in the same year. We consider both droughts as one to conduct the comparison year by year (drought with the identifier (Id) no. 9). We found a total of 21 droughts for the period 1901 to 2013. Columns 4 and 5 of Table A1 show the source of where each drought was originally analysed. Due to the lack of detailed information on the onset and the end in time, we carried out visual inspection of the spatial sequence of drought areas to determine this information for each of the 21 droughts (Figs. A1 to A3, Appendix A). The onset in time was chosen as the month where the beginning of the drought area increase is observed. Similarly, the end was selected as the month where such an area ends up growing. In each reported drought, when there was any difficulty in assigning the onset (end), the reason was indicated in Table A1. When two or more areas were observed at the same time step, the onset (end) was proposed based on the largest one. In these cases of more of one area, a recommendation was given to consider or not the drought's information in the procedure of parameters' selection (Table A1).

The four parameters a, b, c, and d were set by means of a two-step procedure described as follows.

- (1) Calibration (selection): with different combinations of four parameters, the onset and the end of calculated droughts were obtained after the application of S-TRACK method following the procedure indicated in Sect. 2.1.2. Calibration step was performed with a sub-sample of the reported droughts. The number of times (hits) that the computed and catalogue-based onsets and ends agree was calculated. We selected the quartet of parameters that retrieved the most hits.
- (2) Validation (verification): for a second sub-sample of reported droughts, the comparison of their onsets and ends was performed using the parameters selected in the previous step. This second phase allowed us to confirm the suitability of the selected parameters to represent the most droughts.

From the catalogue of 21 reported droughts (Table A1), we considered eight for Calibration and eight for Validation step. Droughts considered for the Calibration are almost all before the 1960s, and those for the Validation are after the 1960s. Five droughts were not considered in this process due to the reasons shown in Table A1. The parameters a and b were considered as qth percentiles of the drought area, whereas the parameters c and d as qth percentiles of the distance between centroids. Although considering the parameters as percentiles allows us to take values from 0 to 100, the intervals were selected based on the order of magnitude of the drought areas and distances. In this way, the following

intervals were chosen for the Calibration-Validation procedure: *a* from 10 to 50, *b* from 50 to 90, *c* form 50 to 90, and *d* from 50 to 90.

2.3.3. Analysis of drought paths and characteristics

Drought paths and drought characteristics were analysed in two parts: (1) the patterns of all paths of droughts for the whole period 1901–2013 (Sect. 3.3.1), and (2) the patterns of the most severe reported droughts (Sect. 3.3.2). We select for the second part of the analysis the droughts of 1905, 1965, 1972, 1987, 2000, and 2002, based on their severe impacts reported.

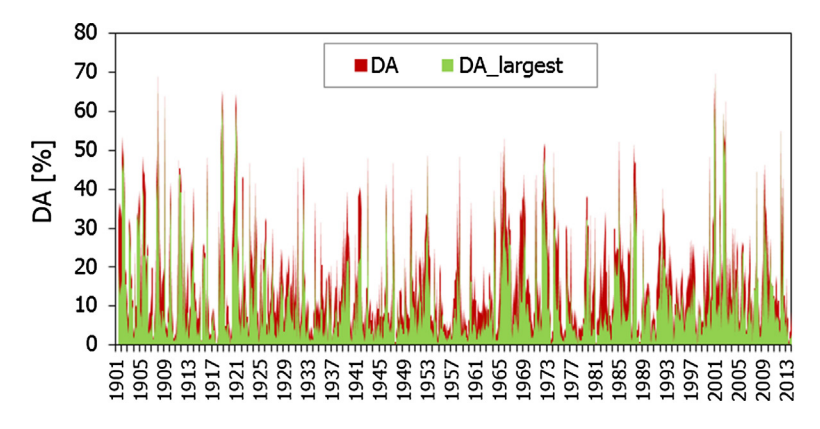
3. Results

3.1. Drought areas

Fig. 2 (left) shows the area of all cells in drought (DA) and that of the largest cluster (DA_largest) for the period 1901–2013. In the extreme cases (maximum and minimum values) DA_largest is more or less similar to DA. The Pearson correlation coefficient (R) was calculated for four intervals of DA_largest presented in Fig. 2 (right). The best R coefficient was observed in the intervals of DA_largest ≤ 10 and DA_largest $\geq 50\%$, i.e. the small and large areas. The lowest R coefficient was obtained for DA_largest between 10 and 30%. Results indicate that for DA_largest values greater than or equal to 30%, DA_largest and DA are very similar. Therefore, it was found that the area in drought of the larger cluster is a good proxy for monitoring the drought area of the region.

3.2. Parameters selection for the spatial tracking algorithm

Fig. 3 shows the number of hits obtained in the Calibration step for the combinations of the four parameters. A hit refers to the simultaneous coincidence of the onset and the end in time of reported droughts (Table A1) and those calculated with the drought tracking algorithm. In Fig. 3, the number of hits is displayed from 1 to 8, where 8 indicates a perfect match. Each number of hits is represented by a colour. The results are arranged as follows. Three 3D scatter plots were prepared for the parameter a = 30, 40, and 50 percentile. In each graph, the horizontal axes correspond to b (50 to 100) and c (50 to 100), whereas the vertical one to d (50 to 100). To display the results in Fig. 3, the parameter intervals were selected to show the subset of the parameter space where the maximum number of hits was found. It was observed that more than one combination of parameters produced the same number of hits. According to the maximum number of hits, we selected the following parameters: a = 40, b = 50, c = 50, d = 90



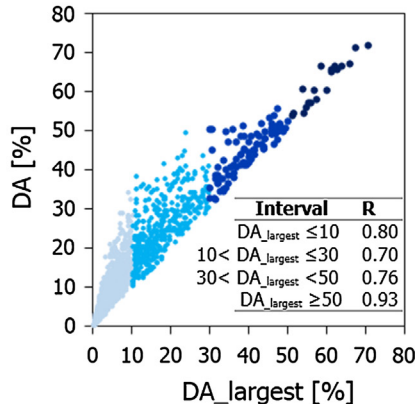


Fig. 2. Percentage of drought area in India considering all cells (DA) and only those of the largest cluster (DA_largest) for period 1901–2013 (left), and scatter-plot of DA_largest vs. DA (right). Pearson coefficient (R) is indicated for four intervals of DA_largest.

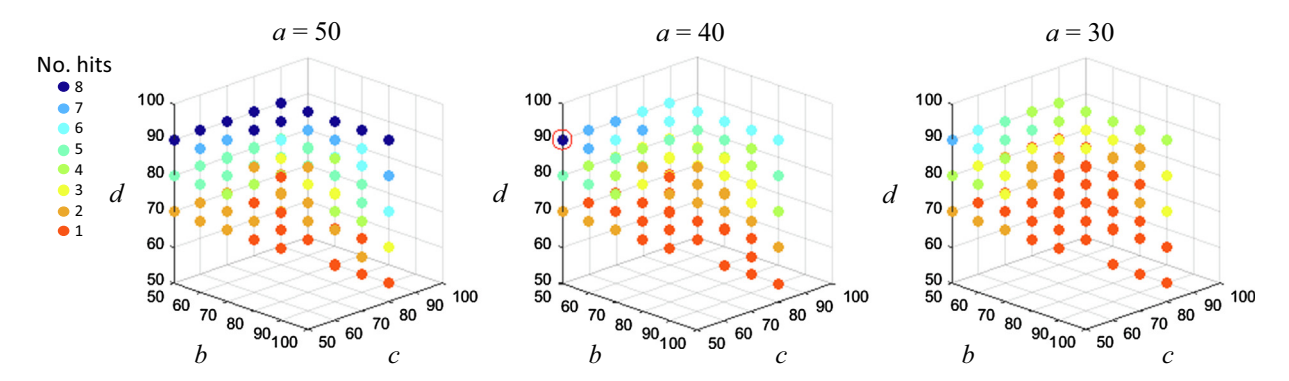


Fig. 3. Number of hits between onsets and ends from calculated and reported droughts (max. 8) for different combinations of parameters *a, b, c* and *d*. The selected combination is indicated with a red circle (centre). (For interpretation of the references to colour in this figure legend, the reader is referred to the web version of this article.)

Table 1

Difference in months between the calculated onsets and ends, and those based on the catalogue of droughts in India (Table A1) for the Calibration (left), and Validation (right) procedure.

Calibration						Validation						
From catalogue Onset End		Calculated Onset End		diff. in onset	diff. in end	From catalogue Onset End		Calculated Onset End		diff. in onset	diff. in end	
1905/6	1906/5	1905/6	1906/5	0	0	1965/5	1966/5	1965/5	1966/5	0	0	
1911/7	1912/2	1911/7	1912/2	0	0	1966/7	1967/2	1966/7	1967/2	0	0	
1915/7	1916/1	1915/7	1916/1	0	0	1972/4	1973/6	1972/4	1973/7	0	1	
1918/4	1919/2	1918/4	1919/2	0	0	1979/8	1980/2	1979/9	1980/2	1	0	
1920/6	1921/7	1920/6	1921/7	0	0	1993/6	1993/12	1993/7	1994/1	1	1	
1942/10	1943/3	1942/10	1943/3	0	0	2000/8	2001/6	2000/8	2001/6	0	0	
1964/3	1964/6	1964/3	1964/6	0	0	2002/6	2003/1	2002/4	2002/12	2	1	
1987/6	1988/2	1987/6	1988/2	0	0	2009/6	2010/1	2009/6	2010/1	0	0	

(Fig. 3 (centre)), although a = 50 and b = 50 produces the same number of hits (Fig. 3 (left)). We chose the former combination because parameter a must be less than b. Table 1 shows the calculated and catalogue-based onsets and ends, as well as their differences for both Calibration and Validation steps. The difference in months was minimal for most of the droughts, even in the Validation step. Only in one of the eight droughts, the difference in onset and end was more than one month.

3.3. Drought paths and characteristics

The analysis of the paths and characteristics of the droughts was carried out in two parts: (1) the entire period of analysis (historical overview) (Sect. 3.3.1), and (2) the worst years in drought (Sect. 3.3.2). Fig. 4 shows the way in which the drought analysis is organised. The number of droughts is pointed out in brackets in each case.

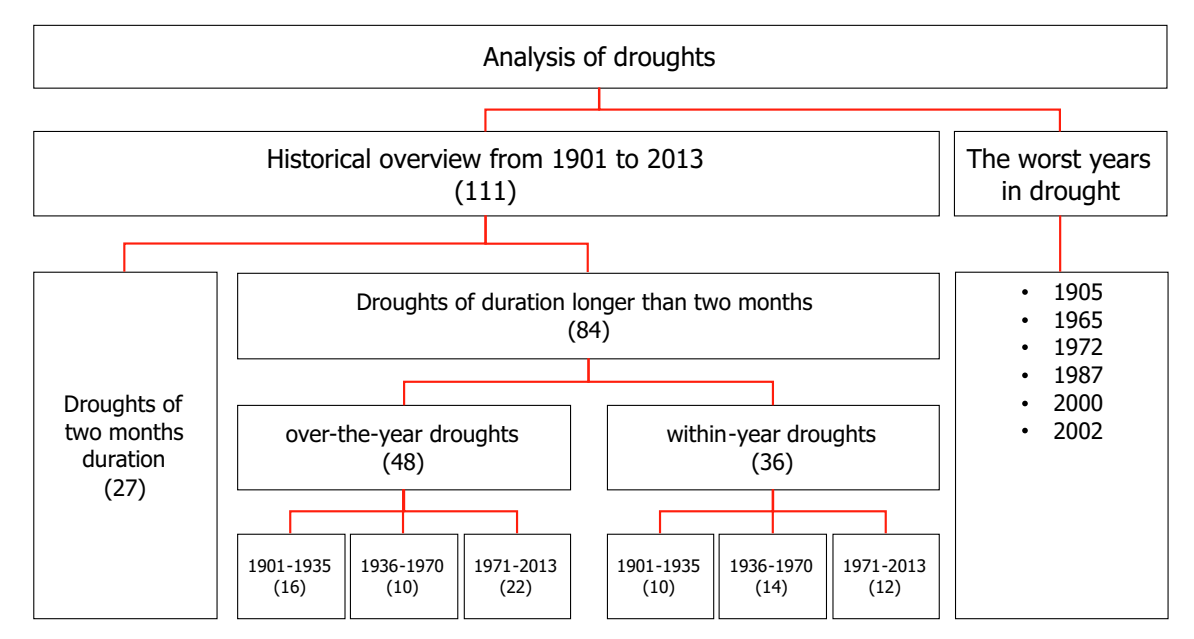


Fig. 4. Schematic overview of the way in which the analysis of droughts is organised. In brackets, the number of droughts is indicated.

3.3.1. Historical overview

In the period 1901–2013, a total of 111 droughts were identified. Of this total, 27 had a duration equal to two months, and 84 lasted longer than two months. Firstly, the results of the two-month droughts are described in the following paragraph. After, the results of those of more than two months are presented.

Of the two-month droughts, 70% occurred in the first semester and 30% in the second semester of the year (Table A2). Of the droughts that occurred in the first part of the year, the intensity was 12.9%/month, i.e. 12.9 percent on average per month. The average length of paths was 8.8 km. For the second half, they were 7.4%/month and 2.9 km, respectively. It was found that 9 out of 19 (47%) droughts of the first semester started and ended in similar locations. In the case of the droughts of the second semester, 7 out of 8 (88%) do so (Table A2). Judging by the occurrence of the two-month droughts shown in Fig. A4, it seems that some of them were remnants or starts of others with longer durations.

The droughts lasting more than two months were analysed in two groups. A difference has to be made between droughts that start and end in different years and those that do so in the same year, named here as over-the-year and within-year droughts, respectively, in a similar way as Arena et al. (2006). The over-the-year and within-year droughts presented different patterns. In this research, drought is considered as over-the-year, even if its duration is less than 12 months.

Furthermore, the analysis period was split into three sub-periods: 1901–1935, 1936–1970, and 1971–2013 following the

results of Mallya et al. (2015). They reported that there was a different behaviour of the meteorological drought in each of the three periods over the study region. The length of paths, duration, severity and intensity of the over-the-year droughts are shown in Fig. 5, and those of the within-year droughts are presented in Fig. 6.

Regarding the over-the-year droughts, Fig. 5 (upper left) shows a significant linear relationship between the duration and severity (Table A3). The slope of the duration-severity line was greater in the first period 1901-1935, following that of the period 1936-1970. The lowest slope corresponds to the third period 1971-2013. The average of duration (in months), and severity (in percentage) were 9.8 and 238 for the period 1901-1935; 9.9 and 184.8 for 1936-1970; and 9.6 and 174.1 for 1971-2013. It was observed that the average duration almost remains unchanged over the three periods, whereas average severity gradually decreases from the first to the third period. This reduction in severity across the three periods explains the decrease in the slope of the duration-severity line. The slight decrease in average duration in the period 1971–2013 was due in part to the presence of more droughts with short durations (less than 10 months), as Fig. 5 shows (upper panels). Droughts with longer durations were more present in the periods 1901–1935 and 1971–2013. A smaller number of droughts was observed in the period 1936-1970. Fig. 5 (upper right) points out that the intensity increases proportionally to the duration. After a certain duration, the intensity decreases instead of increasing. This pattern was observed in the three periods. It was appreciated that the proportional increase in intensity

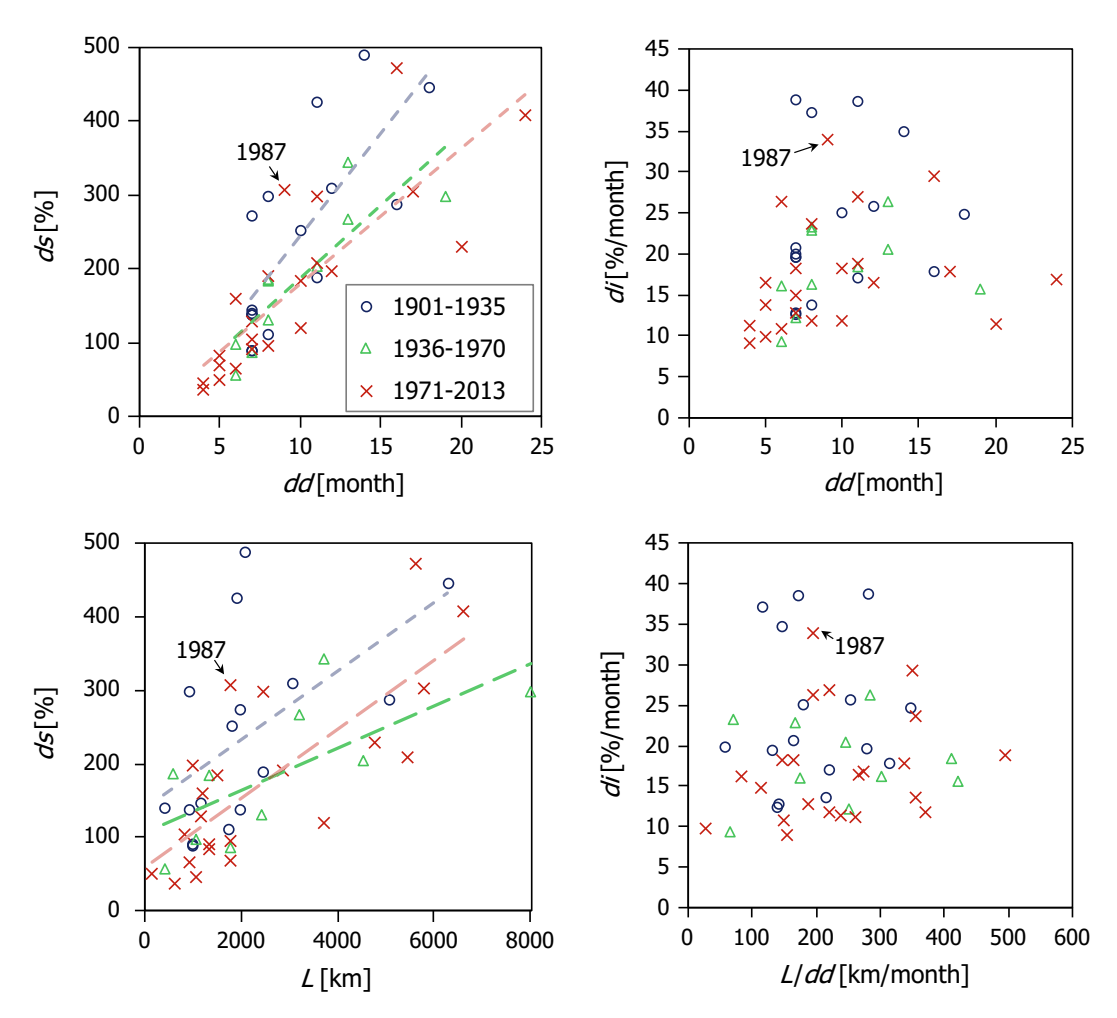


Fig. 5. Length of the path (*L*), severity (*ds*), intensity (*di*), and duration (*dd*) of the over-the-year droughts in India (1901–2013). This figure is accompanied by a significance test for linear regression shown the Table A3.

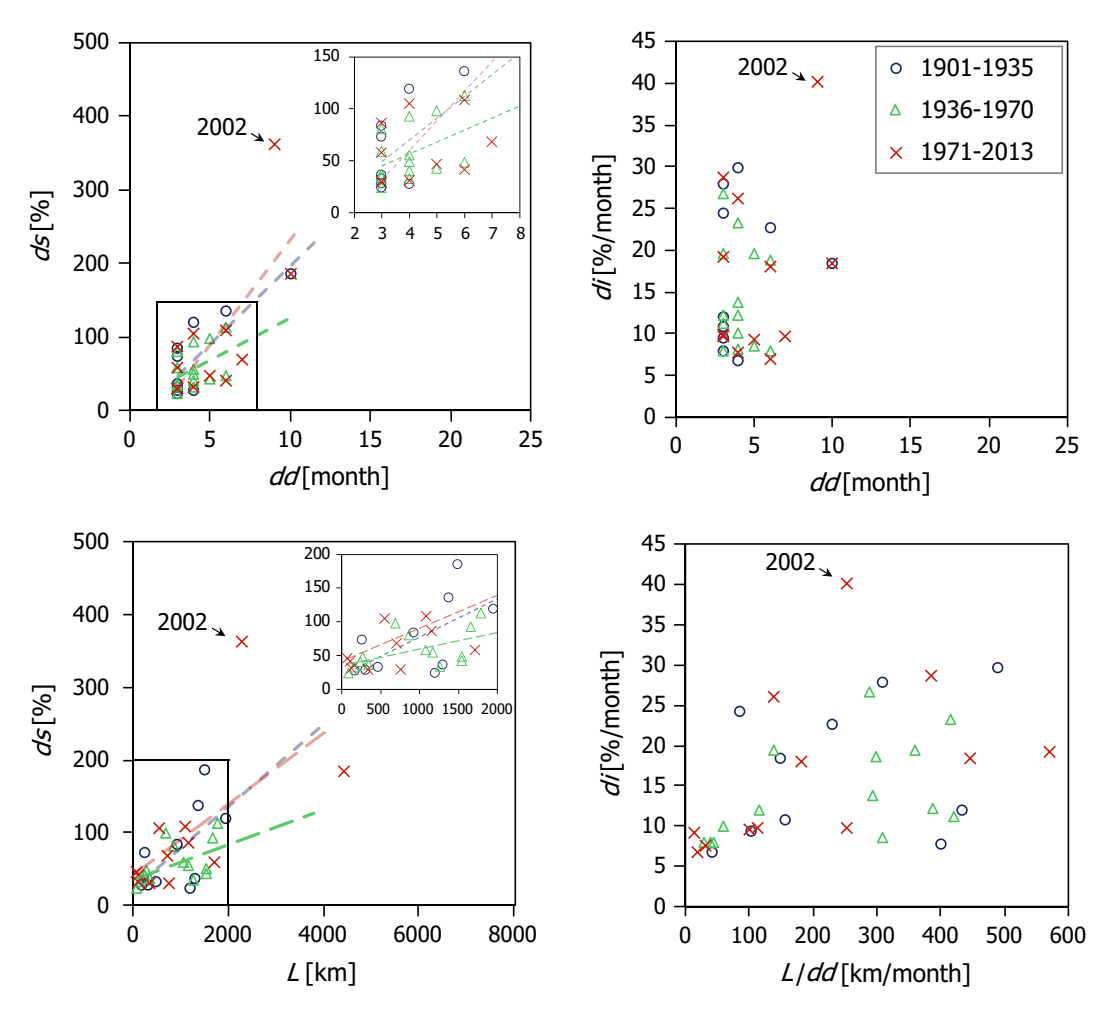


Fig. 6. Length of the path (*L*), severity (*ds*), intensity (*di*), and duration (*dd*) of the within-year droughts in India (1901–2013). This figure is accompanied by a significance test for linear regression shown in Table A3.

occurs for durations of less than 12 months. The average intensity for the period 1901–1935, 1936–1970, and 1971–2013 was 23.7. 18.1, and 17.3%/month, respectively. Fig. 5 (lower left) allows seeing that the severity also increases proportionally to the total length of the paths (Table A3). The slope of severity-length line of the period 1901-1935 was similar to that of the period 1971-2013, with the difference that in the last period the severity was lower for the same length compared to the first period. It seems that the slope of the severity-length line was lower in the period 1936–1970. The average length was 12.3, 14, and 11.1 km for the period 1901-1935, 1936-1970, and 1971-2013, respectively. Fig. 5 (bottom right) indicates that droughts with higher intensities had a length-duration relationship between 100 and 300 km/month (~1 to 3 degree/month). In the over-the-year droughts, it was found that the longer the drought, the larger the length of the path for the three periods (Table A3).

Respecting the within-year droughts, results are presented in Fig. 6 in a similar way to Fig. 5. The severity and duration relationship did not appear to be strongly linear in these droughts as Fig. 6 (upper left) and Table A3 point out. The average duration (in months) and severity (in percentage) were 4.2 and 74.4 for the period 1901–1935; 4.1 and 57.4 for 1936–1970; and 5.3 and 95.7 for 1971–2013. Fig. 6 (top right) reveals that there is no linear relationship between intensity and duration. The highest intensities were observed in the periods 1901–1935 and 1971–2013. The average intensity for the period 1901–1935, 1936–1970, and

1971–2013 was 17, 14.3, and 17%/month, respectively. In general, the linear relationship between severity and length of the paths was not found (Fig. 6 (bottom left) and Table A3). The average length for the period 1901–1935, 1936–1970, and 1971–2013 was 8.3, 8.8, and 10.3 km, respectively. In Fig. 6 (bottom right), a drought was observed with considerable intensity. This drought occurred in 2002. According to Guha-Sapir (2018), the most severe historical droughts over India were 1987 and 2002. The results indicated that both droughts showed similar intensities, durations, and lengths of the paths: 34%/month, nine months, and 1,761 km for the 1987 drought; and 40.2%/month, nine months, and 2,271.4 km for the 2002 drought. In within-year droughts, it was not found a linear relationship between the length of path and duration, in general (Table A3).

Fig. 7 presents the relative frequency of three characteristics of the over-the-year droughts. These characteristics are month of onset and end, initial and final location, as well as rotation. Regarding the month of onset, it was observed that in the periods 1901–1935 and 1936–1970, droughts started in the second semester, while in the third period (1971–2013), they started in the second, and first semester. The months with greater frequency for the period 1901–1935 were June and July, while for 1936–1970 they were August and July. In the period 1971–2013, August seems to have a frequency slightly higher than the other months. About the month of the end, this seems to fell in the first semester in each of the three periods. In addition, for the period 1901–1935, February

and April were the months with the greatest frequency; in 1936-1970, they were February and June; and for 1971–2013, they were February and April. On the other hand, in the period 1901-1935, the initial locations appear to be the south, west and centre; the south and west in 1936-1970; and the south, east and north in 1971-2013. The final location in 1901-1935 was the south; the centre in 1936-1970; and in the last period (1971-2013), no predominant final location was identified. The relative frequencies of the pathways (routes) are displayed in Figs. A5 to A7, for each period, respectively. In 1901-1935, south-to-south, west-tosouth, and centre-to-centre pathways presented the highest relative frequencies; in 1936-1970, south-to-centre did so; and in 1970–2013, there was no predominant route observed. The occurrence of droughts with pathways with a similar initial and final location, for example south-to-south in the period 1901-1935 (Fig. A5), is maybe associated with droughts that grow by expanding their spatial extent and then shrink while maintaining their location in a particular site. In all three periods, this type of behaviour was observed. Finally, about to rotation, the relative frequency of mostly clockwise was slightly higher in the period 1901–1935, while in the periods 1936–1970 and 1971–2013, it was mostly counter-clockwise.

Similar to Fig. 7, Fig. 8 displays the relative frequency of the onset and end month, initial and final location, as well as rotation of the within-year droughts. The month of onset was mostly located in the first three quarters of the year in all three periods. May was the month with the highest relative frequency for the period 1901–1935; May and August for 1936–1970; and May and February for 1971–2013. Moreover, the month of the end with the highest frequency for the period 1901–1935 was April; June and November for 1936–1970; and May and November for 1971–2013. Concerning the initial location, in the period 1901–1935, the north had the highest frequency; the south and east in 1936–1970; and the east in 1971–2013. Regarding the final location, for 1901–1935, there was no predominant one identified; for 1936–1970, it was observed that the north and east had the

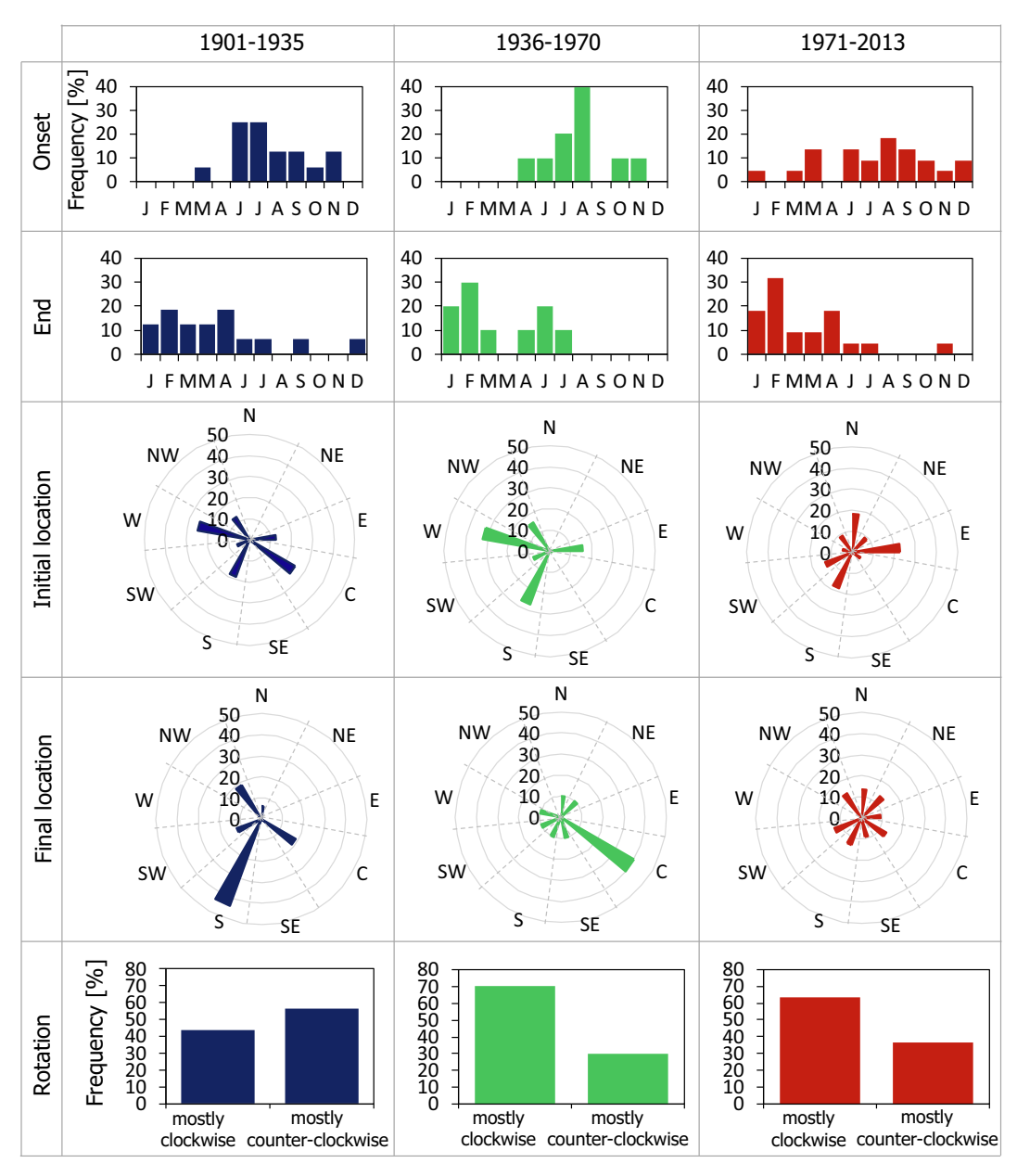


Fig. 7. Relative frequency of onset, end, initial and final location, as well rotation of the over-the-year droughts in India (1901-2013).

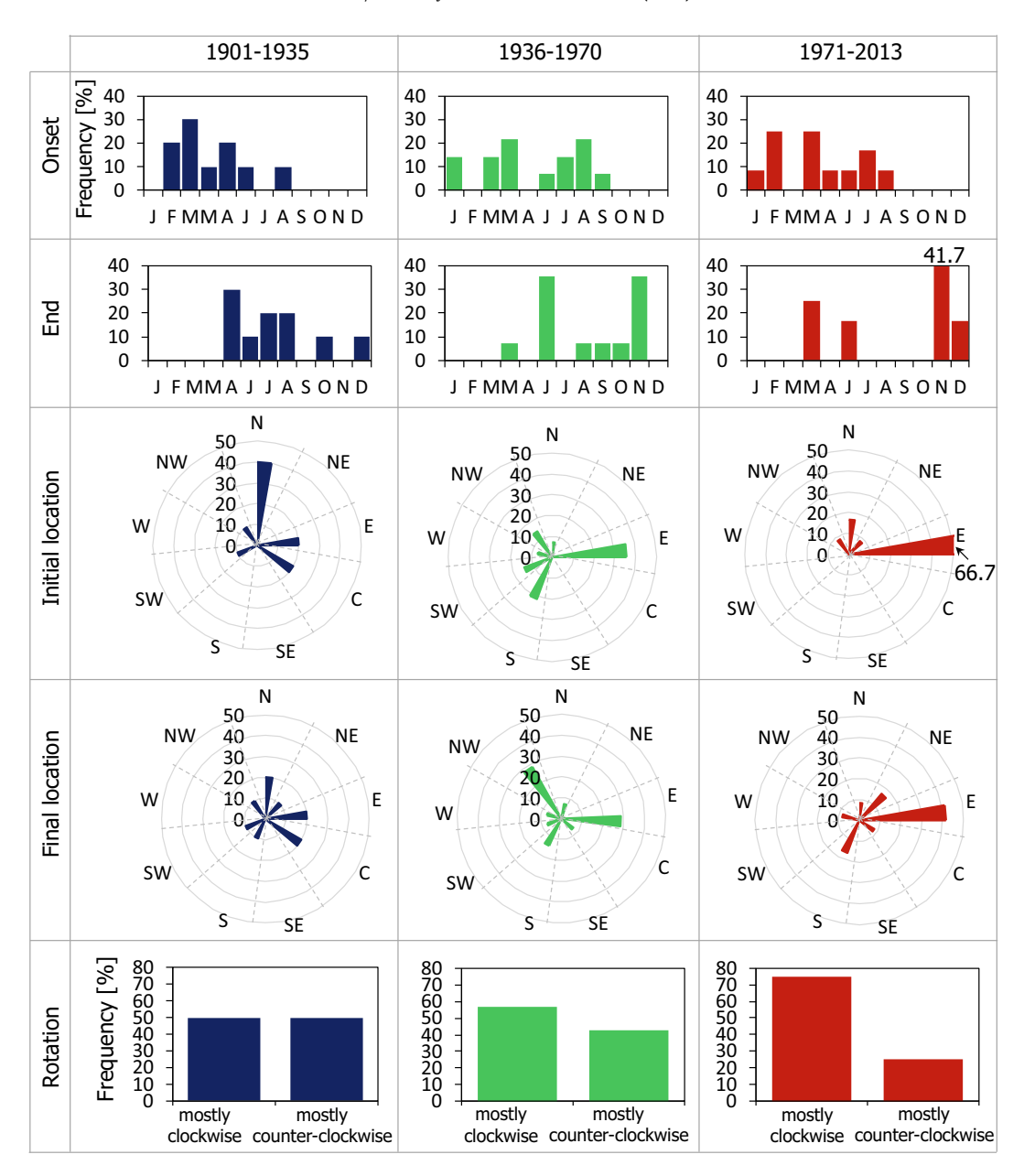


Fig. 8. Relative frequency of onset, end, initial and final location, as well rotation of the within-year droughts in India (1901-2013).

highest frequency; and for 1971–2013, the east did so. Figs. A8 to A10 present the relative frequencies of the pathways (routes) of the droughts for the periods 1901–1935, 1936–1970, and 1971–2013, respectively. In the period 1901–1935, the north-to-north pathway showed a higher relative frequency; and east-to-east pathway did so for 1936–1970 and 1970–2013. Apparently, the pattern where the initial and final location are similar had the highest frequencies in all three periods. As mentioned, this pattern may indicate that droughts grow by expanding their spatial extent and then shrinking at a certain magnitude in particular site. Finally, regarding the rotation, for the periods 1901–1935 and 1936–1970 a predominant pattern was not identified. In the period 1971–2013, it was observed that mostly counter-clockwise frequency was predominantly superior.

3.3.2. The worst years in drought

Paths of the most extreme years in drought (1905, 1965, 1972, 1987, 2000, and 2002) in India are presented in Fig. 9. In all cases,

drought areas overlap considerably in the last time steps, which suggests that the spatial extent after reaching a considerable size, maybe it remains more or less in the same region. The staying of large drought areas in the same region over time may explain the severity of droughts in these years, and hence these were reported because of their impacts. For the most severe reported droughts (1987, 2002) a pattern was detected: it was observed that drought areas in the initial phase moved around, but then overlapped considerably at the end. In terms of spatial extent, 2000 and 2002 droughts were the largest. In Fig. 9 the average of intensity, duration, length of the path, and rotation are provided for each drought.

Of the droughts shown in Fig. 9, with an intensity of 40.2%/month, the 2002 drought had the highest value. The intensities range between ~ 25 and 40%/month; the durations between 9 and 16 months; and the lengths between $\sim 2,000$ and 5,500 km. The length and duration rate run between ~ 200 and 350 km/month. It was noted that the rotation (dr) for the 1905 and 1965 droughts

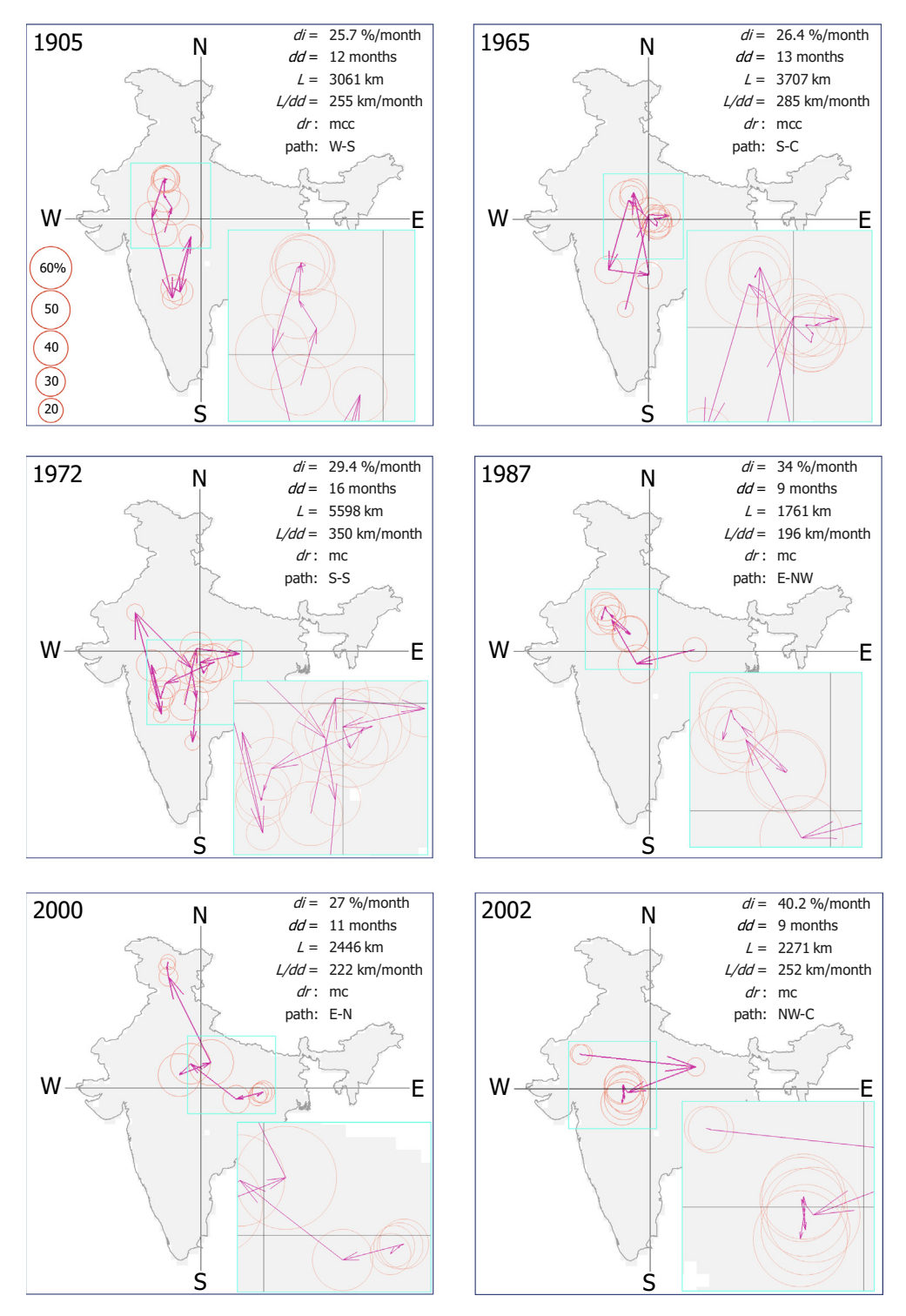


Fig. 9. Drought paths (red arrows) of selected years with the most severe droughts in India, incl. the drought characteristics (Sect 2.1). *di, dd, L, dr*, mc, and mcc stand for intensity, duration, length of the path, rotation, mostly clockwise, and mostly counter-clockwise, respectively. Spatial drought extent is schematised by a circle where its centre corresponds to the respective centroid and its size to the percentage of drought area with respect to India. Insets show zoomed-in views. For the sake of clarity, a reduction factor was used to show the circles. Circles shown in the upper left panel indicate the magnitude of the drought area in percentage. The origin of the axes is placed in the centre of the country. (For interpretation of the references to colour in this figure legend, the reader is referred to the web version of this article.)

was mostly counter-clockwise (mcc) and for those of 1972, 1987, 2000, and 2002, it was mostly clockwise (mc). There was no predominant route followed by droughts in these years, but it seems that the regions where the centres of the worst ones were located are the west, south, and centre for droughts of 1905, 1965 and 1972, while the north, east, and centre for the ones of 1987, 2000 and 2002.

4. Discussion

4.1. Droughts in India

Results of location, intensity, and duration of calculated droughts are discussed in this paragraph. Previous studies conducted in India were consulted and analysed to compare the findings of this research. The zones where the droughts have most frequently occurred, apparently have not been the same throughout the period of analysis. This has also been reported in other studies. For example, Mallya et al. (2015) found that in the period 1901-1935, a greater number of cells in drought were located in the south and centre; in the period 1936-1970, it occurred in the east; and in the period 1971-2004, it was in the east and centre. They also found that in the period 1936-1970, the percentage of the drought area was lower than in the other two periods. In the same way, Naresh Kumar et al. (2012) reported an increase in the number of cells in drought in the 1970 s, 1980 s, 1990 s, and 2000 s. They also pointed out the years where the cells in drought showed a high persistence, i.e. cells in conditions of continuous drought. These years were 1984, 1972, 1974 and 2002. Additionally. Mishra et al. (2016) found an increase in the drought areas in the period 1960-2000 compared to those of the period 1920-1959. Regarding the duration of droughts, Mallya et al. (2015) reported the longest ones in the 1971-2004 period, after 1901-1935, and finally 1936-1970. Results shown in Figs. 5, 6, 7, and 8 are in line with the findings of Mallya et al. (2015), Naresh Kumar et al. (2012), and Mishra et al. (2016). It seems that the drought patterns of the first third of the 20th century and the last one are more or less similar in terms of intensity and duration.

In relation to the onset and end location, as well as the rotation of calculated droughts, it was not found a similar study for India. In this case, results were discussed considering the researches concerning the monsoon precipitation (June to September) in India, which is the main amount of annual rainfall. Monsoon precipitation represents about 80% of the annual total. Some authors have reported that since 1950 there has been a decrease in the amount of this seasonal rainfall (Mishra et al., 2016). Apparently, in contrast, Goswami et al. (2006) reported an increase in the frequency of extreme rain events and a significant decrease in the frequency of moderates for the same period. They performed an analysis on a daily basis. In general, the results of the daily and seasonal analysis show a decline in the amount of rainfall in the monsoon season. while on the other hand, daily rainfall events have increased in the same period. This suggests that the amount of monsoon rainfall has decreased and its distribution over time changed, concentrating on extreme events.

The reported on the changes in monsoon precipitation and extreme rain events (Mishra et al., 2016; Goswami et al., 2006) can partially explain the change in patterns of the onset and end location, as well as the rotation. During the periods 1901–1935 and 1936–1970, the mentioned characteristics (onset and end location, and rotation) are very similar, but for the period 1971–2013, the patterns seem to have changed. The shift on the patterns of daily and seasonal precipitation were also observed more or less in the same period. This suggest that in a certain way, the decrease

of the rain of the monsoon season as well as its concentration in time, with the consequent increase in the frequency of extreme events of rainfall, has caused a modification in the spatial distribution of the drought areas, which could cause the changes in the indicated patterns. Regarding the most severe years in drought, this shift in the rotation pattern was also observed. The droughts of 1905 and 1965 presented a mostly counter-clockwise rotation (mcc), whereas those of 1972, 1987, 2000, and 2002 shown a mostly clockwise rotation (mc). Moreover, although a predominant onset and end location was not observed, it is identified that in the case of the 1905, 1965, and 1972 droughts, locations were presented mainly in the southwest, while in those of 1987, 2000, and 2002, in general, locations were observed in the northwest.

4.2. Limitations

In this research, for the calculation of the spatial extent of the drought, only the information of the drought indicator was considered. This drought indicator is calculated with meteorological information (precipitation and evapotranspiration). The effects that topography and land use could have on the delineation of drought areas are not taken into account. These factors can be included, for instance, with the use of a drought indicator that evaluates the drought condition on the land surface (e.g. Corzo Perez et al., 2011).

In addition, in this study, a single combination of parameters was used to identify the drought paths for a specific drought indicator. Moreover, a unique drought indicator threshold was used for the calculation of the spatial extent of droughts (Sect. 2.3.1 Drought areas calculation). This threshold is widely used in studies of drought; however, it is suggested to explore other values in future studies.

5. Summary and conclusions

This research presents an application of an approach to describe the way in which drought moves in space, namely drought dynamics. This approach allows the identification of droughts delimited by an onset and an end in time and in space. Paths (consecutive spatial drought tracks), length of path, severity, duration, as well as localisation (onset and end position), and rotation of droughts were calculated. The occurrence of calculated droughts was compared with documented information.

With a calibration–validation procedure, parameters were assigned to the drought tracking algorithm S-TRACK for the identification of spatial drought paths. In the calibration–validation procedure, the onset and end in time of calculated droughts were compared with those inferred from reported droughts.

In the framework of this research, the study of the implications on the choice of different combinations of parameters over the construction of paths and characterisation of droughts was also conducted. The description of such an experiment accompanied by a detailed introduction of the drought tracking algorithm were also prepared for a parallel publication.

Further research is being developed to build a model to predict the spatial drought tracks. This model is based on Machine Learning techniques. Details on this research can be consulted at www. researchgate.net/project/STAND-Spatio-Temporal-ANalysis-of-Drought.

Summary of main findings for India are the following: From the historical overview from 1901 to 2013:

 Location and rotation of the droughts have been changed across the country over time. Some routes by droughts were identified when observing the historical drought paths.

Regarding the worst years in drought: 1905, 1965, 1972, 1987, 2000, and 2002:

- For these years, it is observed that drought areas overlap considerably over time.
- There is no predominant route followed by droughts in these years.
- The part where the worst droughts were located has been not the same over the time.
- For the most severe droughts (1987, 2002), it was detected that both had similar magnitude and duration but shown different paths.
- In terms of spatial extent, 2000 and 2002 droughts showed the largest areas.

Declaration of Competing Interest

The authors declare that there is no conflict of interest regarding the publication of this article.

Acknowledgements

VD thanks the Mexican National Council for Science and Technology (CONACYT), Mexico and Alianza FiiDEM, Mexico for the study grand 217776/382365. HvL is supported by the H2020 ANY-WHERE project, European Union (Grant Agreement No. 700099). The study is also a contribution to the UNESCO IHP-VII programme (Euro FRIEND-Water project), France and the Panta Rhei Initiative of the International Association of Hydrological Sciences (IAHS), United Kingdom.

Appendix A

Table A1

Summary of the catalogue of reported droughts in India. Own elaboration with information from Emergency Events Database (EMD, Guha-Sapir, 2018), Bhalme and Mooley (1980), and Standardized Precipitation Evaporation Index (SPEI)-6 data (http://spei.csic.es/) (Figs. A1 to A3). Cal. and Val. are the abbreviations of Calibration and Validation. The Cal. and Val. columns provide information on years that have been used for the calibration and validation procedure. Some years were not considered, the reason is indicated in each case (Observation column).

# Year	Disaster Id.	Reported in		Based on SPEI-6 drought areas				For parameters selection		
			EMD	B&M	Onset	End	Observation(s)	Cal.	Val.	Not consider
1	1905			х	1905/6	1906/5		х		
2	1911			х	1911/7	1912/2		Х		
3	1915			х	1915/7	1916/1		Х		
4	1918			Х	1918/4	1919/2	There seems to be a short drought from 1918/04 to 1918/06.	х		
5	1920			х	1920/6	1921/7	The end is not clear.	X		
6	1941			x	1941/6	1942/1	Do not consider for Sel. (Eva.). More than one cluster is observed. Onset and end are based on the largest one.			Х
7	1942	1942-9003	х		1942/10	1943/3	Drought with small areas.	х		
8	1951			х	1951/7	1952/2	Difficult to identify onset (end) because of many small clusters.			х
9	1964	1964-9009 and 1964-9044	x		1964/3	1964/6	·	х		
10	1965	1965-9073	X	х	1965/5	1966/5	Onset is not clear.		X	
11	1966			х	1966/7	1967/2	Do not consider for Sel., only for Eva. It is observed more than one cluster. Onset and end are based on the largest one.		х	
12	1972	1972-9073	X	х	1972/4	1973/6	End is not clear.		X	
13	1974			х	1974/3	1975/2	Same as 6.			x
14	1979	1979-9005	X		1979/8	1980/2	Same as 11.		X	
15	1982	1982-9350	Х		1982/7	1983/2	Do not consider for Sel. and Eva. Areas in the sequence are small and widely separated.			x
16	1987	1987-9024	X		1987/6	1988/2		X		
17	1993	1993-9472	х		1993/6	1993/12	Same as 11.		x	
18	1996	1996-9328	Х		1996/6	1997/2	Same as 6.			х
19	2000	2000-9222	х		2000/8	2001/6	Same as 11.		x	
20	2002	2002-9349	х		2002/6	2003/1	Same as 11.		x	
21	2009	2009-9323	х		2009/6	2010/1	Same as 11.		x	

Table A2Summary of statistics of two-month droughts. The number of droughts (*n*), minimum (min), maximum (max), mean, and standard deviation (SD) are presented. In the direction column, the cases when the onset and end location are similar is indicated (*).

	1st semeste	r		2nd semester					
	n=19			n=8					
	min	max	mean	SD		min	max	mean	SD
Intensity [%/month]	7.1	30.1	12.9	6.3	Intensity [%/month]	5.8	10.4	7.4	1.5
Length [km]	0.4	25.9	8.8	8.2	Length [km]	0.2	15.4	2.9	4.7
Number of droughts p	er direction and loca	ation							
Direction	no. of droughts no. of similar Onset and End locations		Direction no. of droughts			no. of similar Onset and End locations			
C to C*	1		9		N to N*	2		7	
C to N	1				NW to NW*	1			
E to E*	4				S to S*	1			
E to N	1				SE to NW	1			
E to S	1				SW to SW*	3			
N to N*	2				Total	8			
NE to E	1								
NW to NW*	1								
NW to S	1								
S to E	1								
S to S*	1								
S to W	1								
SW to N	1								
SW to S	1								
W to C	1								
Total	19								

Table A3Summary of significance test for linear regression at the 0.05 significance level. This table accompanies Figs. 5 and 6. Squared correlation coefficient (R^2) and F-statistic are presented for the three periods shown. They were calculated to investigate the linear relationship between severity and duration (ds vs. dd), severity and length of path (ds vs. L), as well as length of path and duration (L vs. dd). The cases in which there is a significant linear relationship between the variables are indicated (*). The above occurs when F-statistic < significance level (rejection of the null hypothesis).

	ds vs. dd		ds vs. L		L vs. dd		
Period	R^2	F-statistic	R^2	F-statistic	R^2	F-statistic	
over-the-year drou	ghts						
1901-1935	0.58	0.000590*	0.31	0.023733*	0.80	0.000003*	
1936-1970	0.73	0.001571*	0.48	0.025365*	0.88	0.000070^*	
1971-2013	0.67	0.000004*	0.58	0.000036*	0.74	0.0000003*	
within-year drough	nts						
1901-1935	0.71	0.002244*	0.39	0.055464	0.18	0.214882	
1936-1970	0.20	0.109521	0.29	0.046999	0.05	0.462389	
1971-2013	0.52	0.007941*	0.41	0.025330*	0.44	0.018508*	

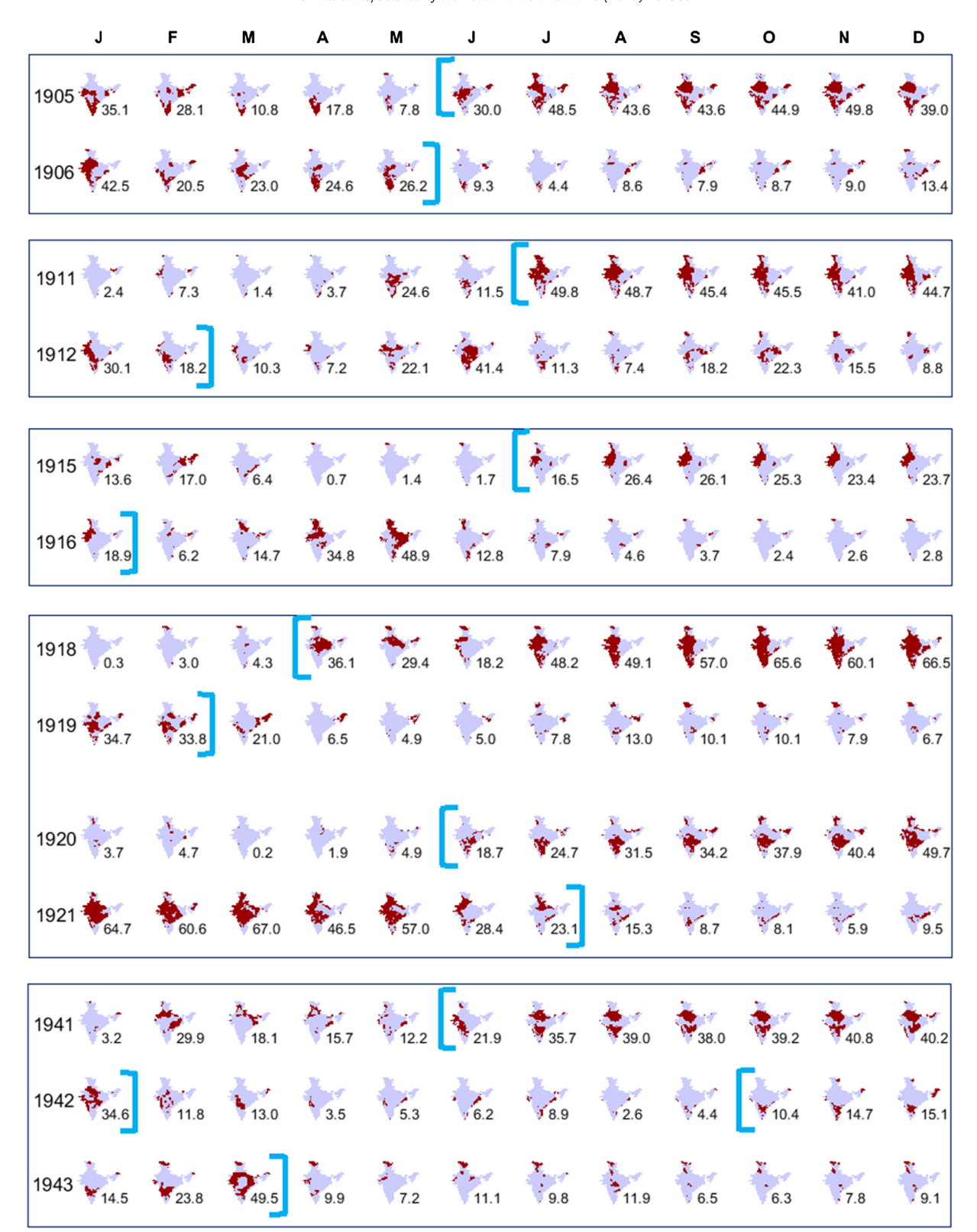


Fig. A1. Monthly drought areas for the years where droughts were reported in the Emergency Events Database (EM-DAT) (Guha-Sapir, 2018) and Bhalme and Mooley (1980). The percentage of drought area is pointed out. It is presented droughts of 1905, 1911, 1915, 1918, 1920, 1941 and 1942. The onset ([) and end (]) are indicated (Sect. 2.3.2 for details).

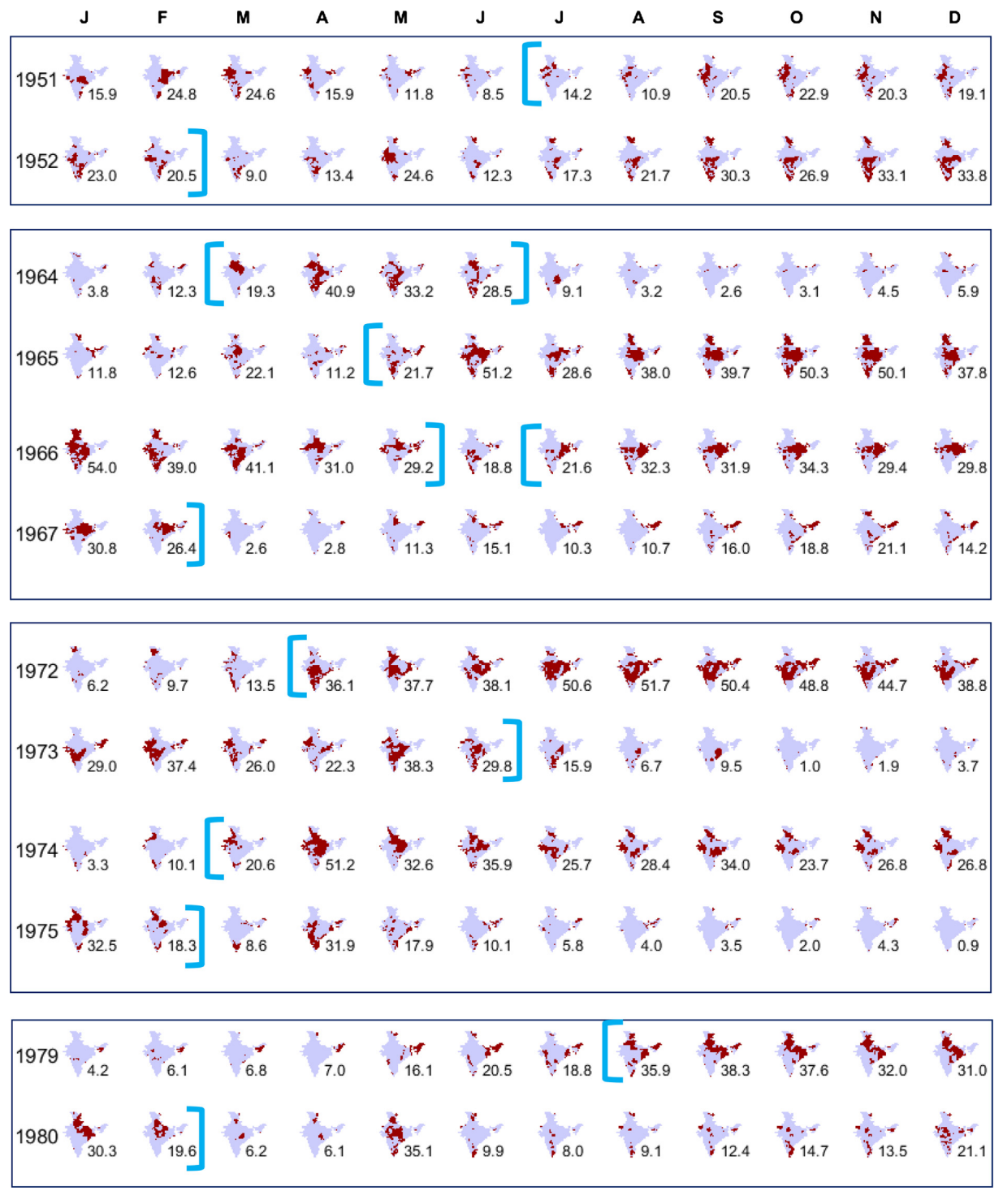


Fig. A2. Same as Fig. A1 but for droughts of 1951, 1964, 1965, 1966, 1972, 1974 and 1979.

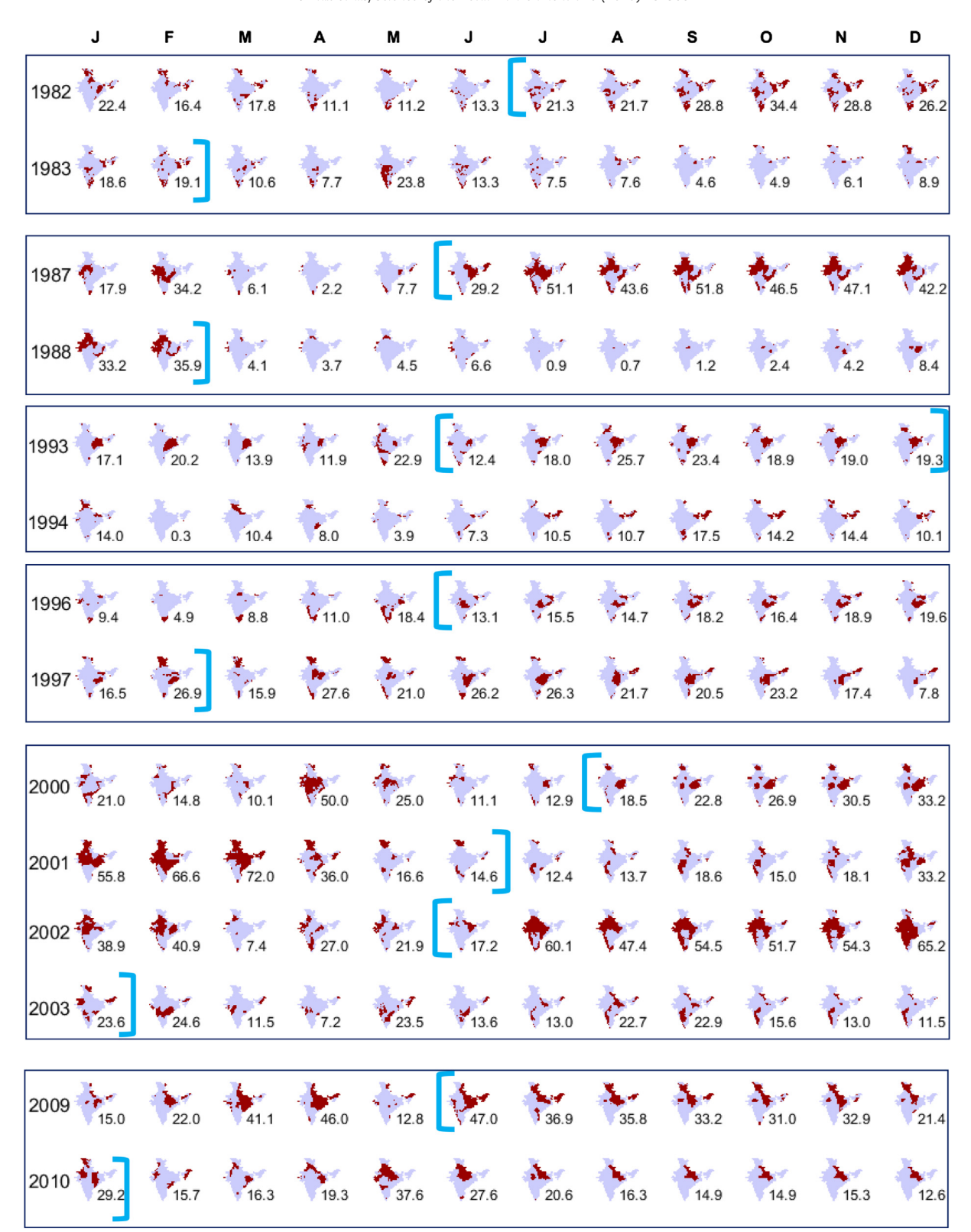


Fig. A3. Same as Fig. A1 but for droughts of 1982, 1987, 1993, 1996, 2000, 2002 and 2009.

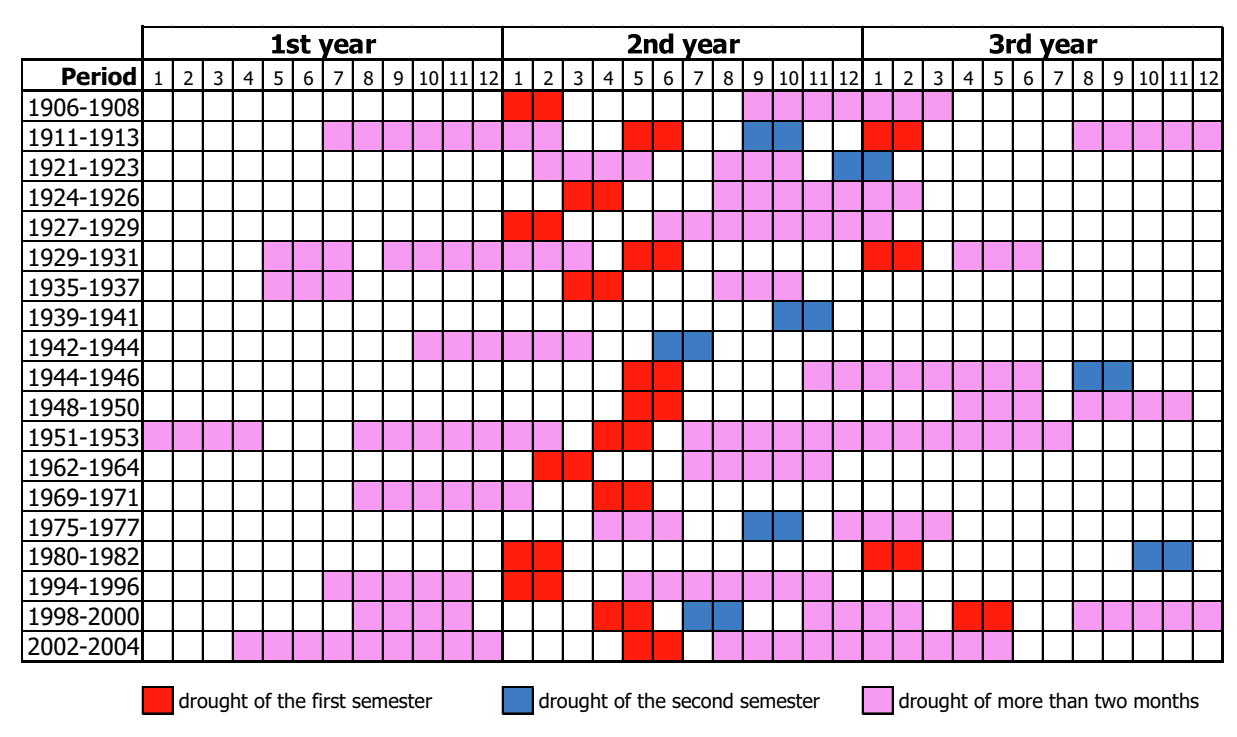


Fig. A4. Droughts of two months duration. Occurrence is indicated for droughts of the first and second semester, as well as for those of more than two months. In each row, months are displayed for a period of three years, from January (1) to December (12). The month from the first to the third year of that period is shown in each column. Some two-month droughts appear to be remnants or starts of droughts of others with longer durations.

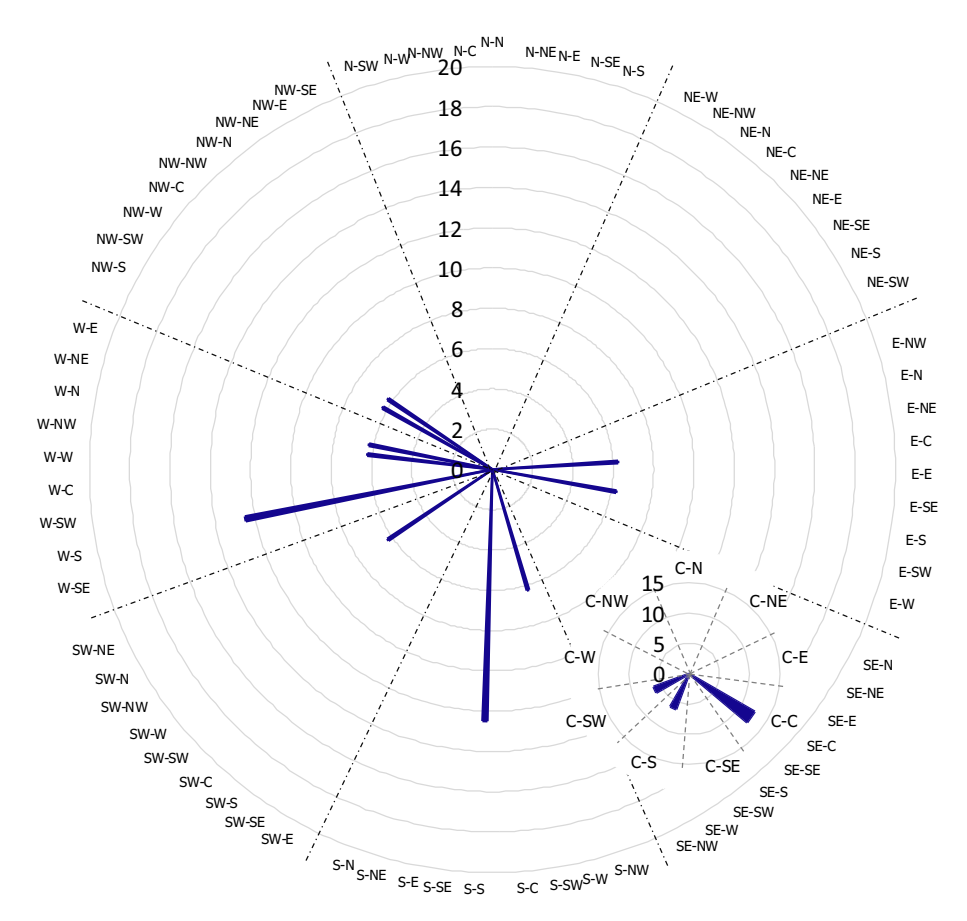


Fig. A5. Relative frequency of path direction of the over-the-year droughts in India (1901–1935).

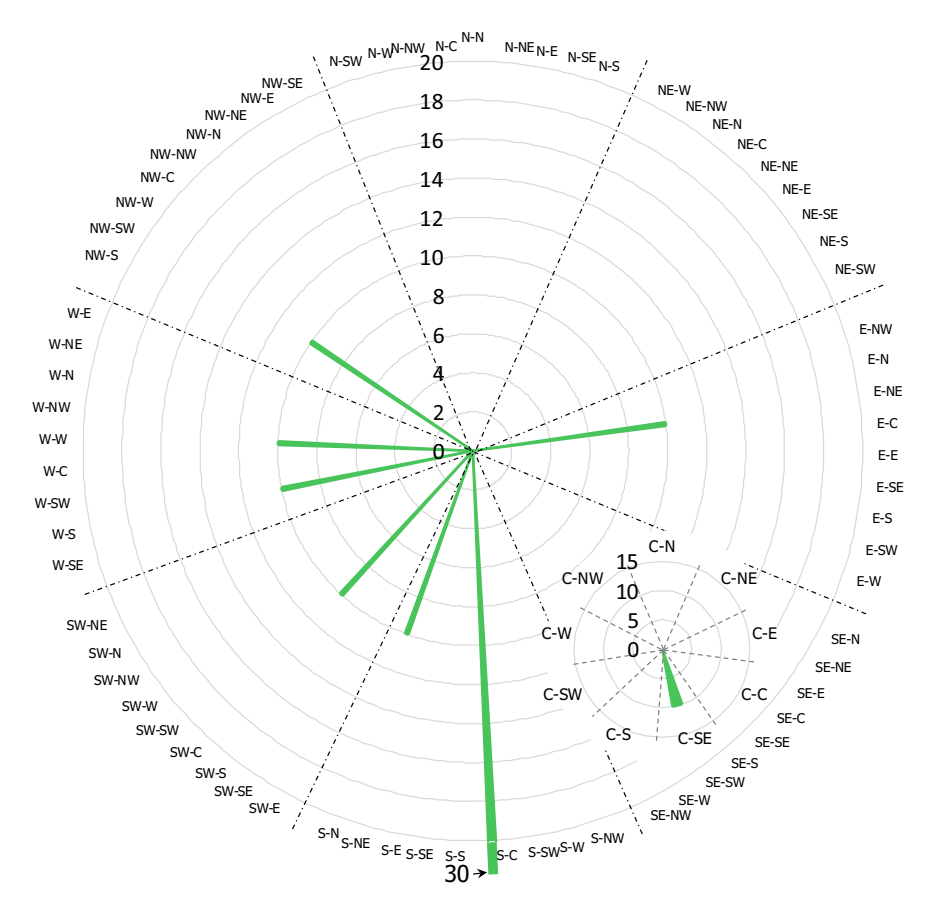


Fig. A6. Same as Fig. A5 but for 1936-1970.

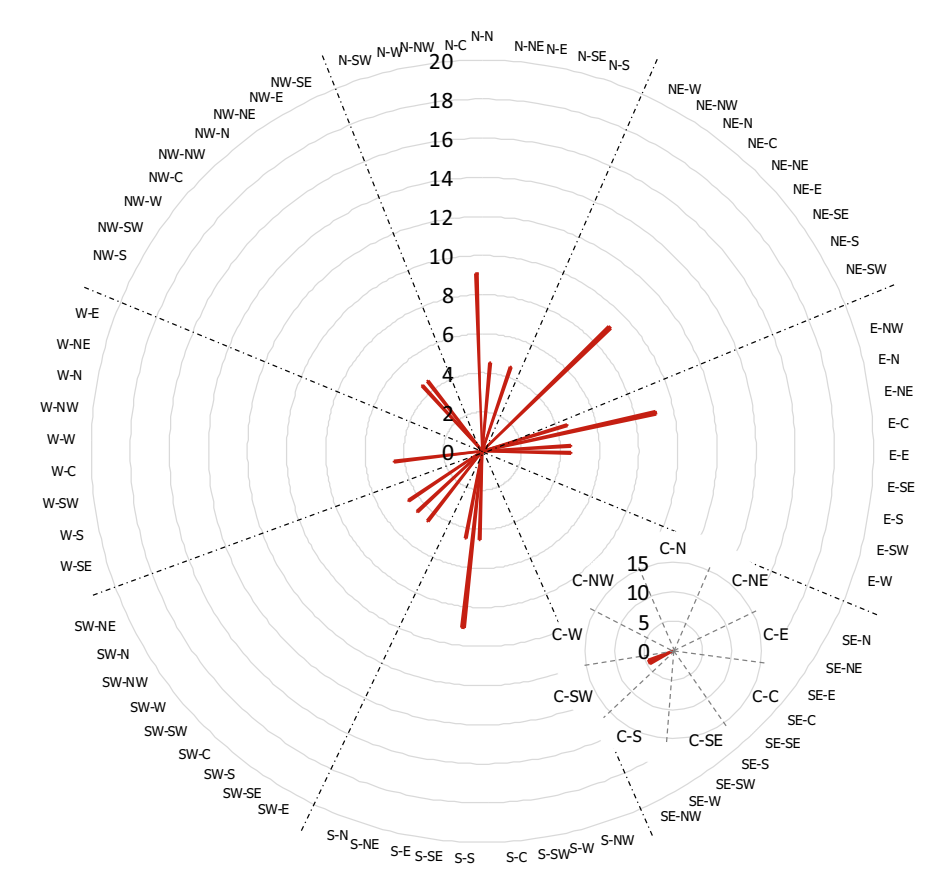


Fig. A7. Same as Fig. A5 but for 1971-2013.

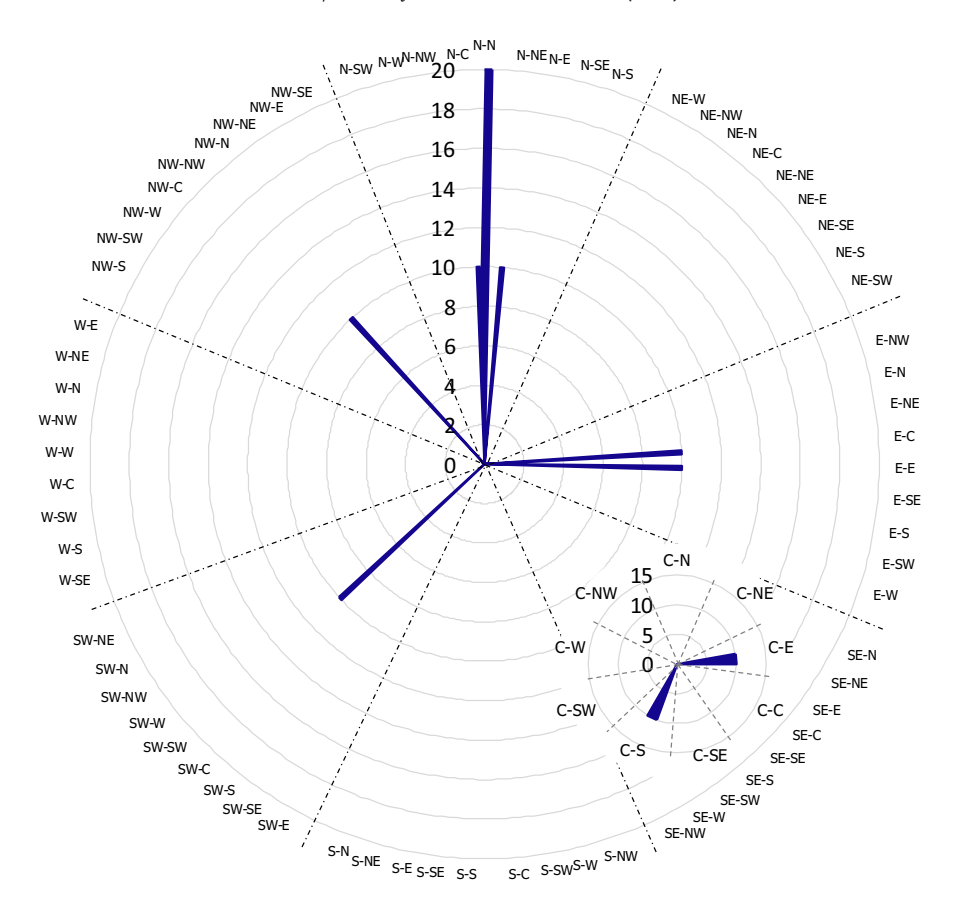


Fig. A8. Relative frequency of path direction of the within-year droughts in India (1901–1935).

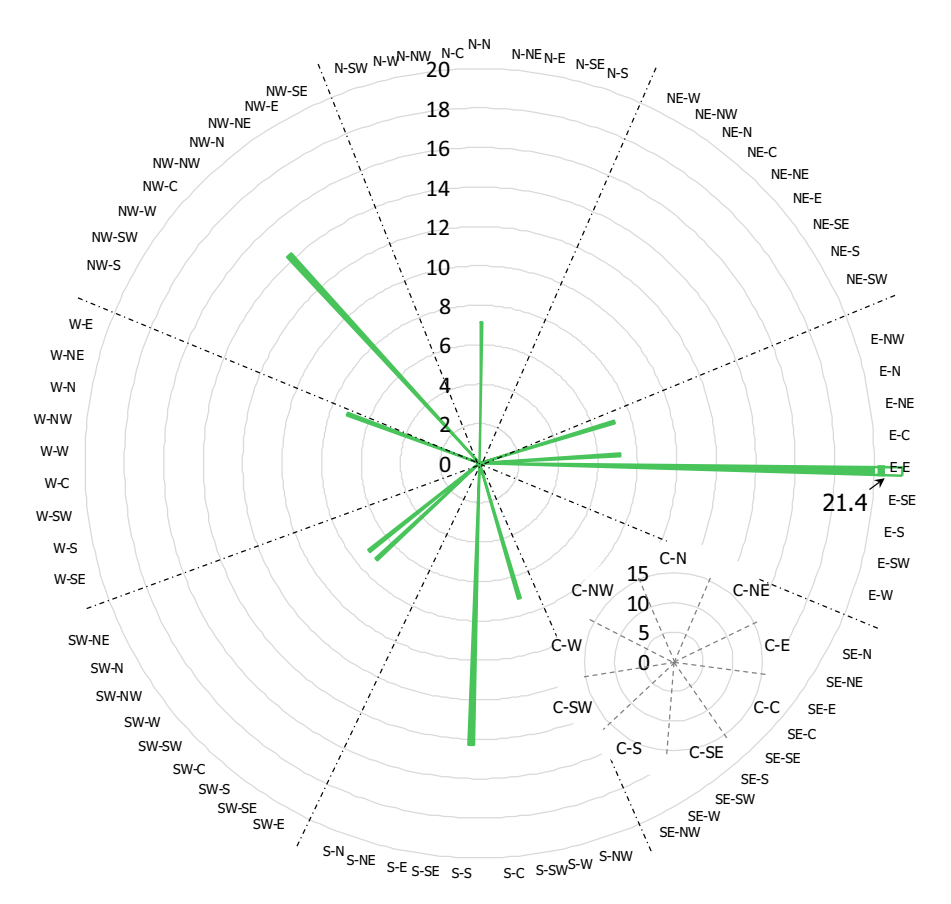


Fig. A9. Same as Fig. A8 but for 1936–1970.

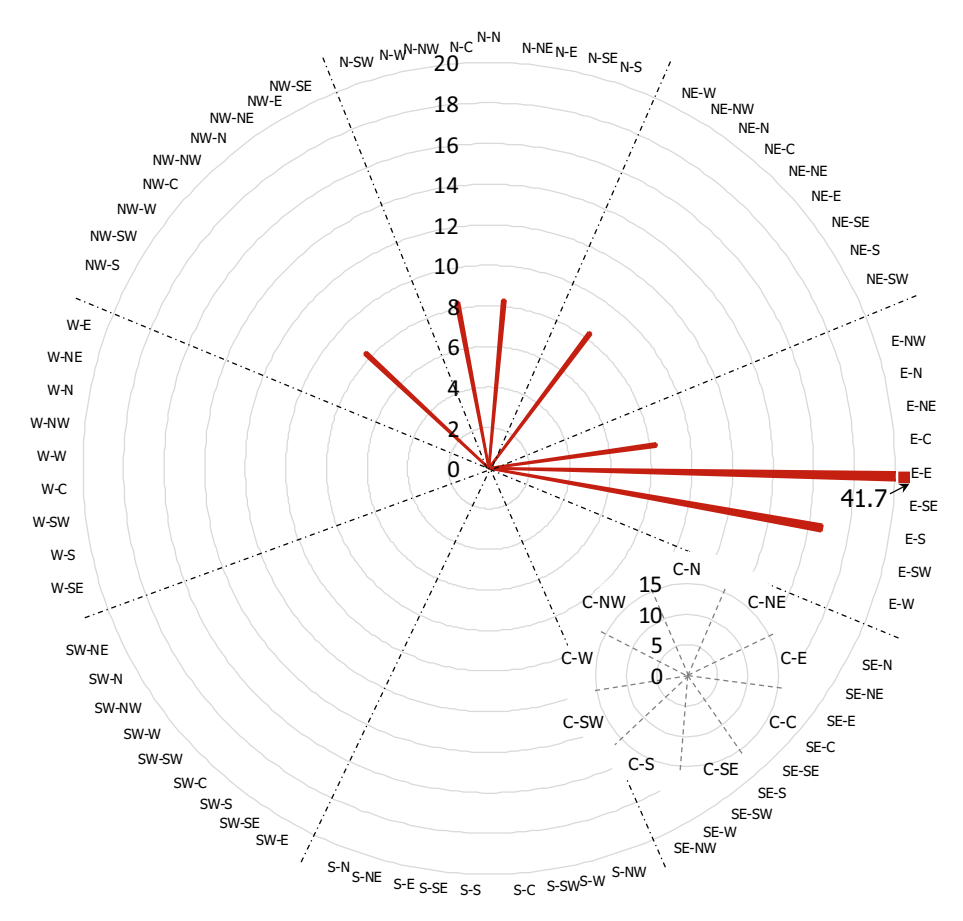


Fig. A10. Same as Fig. A8 but for 1971-2013.

References

Andreadis, K.M., Clark, E.A., Wood, A.W., Hamlet, A.F., Lettenmaier, D.P., 2005. Twentieth-century drought in the conterminous United States. J. Hydrometeorol. 6 (6), 985–1001. https://doi.org/10.1175/JHM450.1.

Arena, C., Cannarozzo, M., Mazzola, M.R., 2006. Multi-year drought frequency analysis at multiple sites by operational hydrology – A comparison of methods. Phys. Chem. Earth, Parts A/B/C 31 (18), 1146–1163 https://doi.org/10.1016/j.pce.2006.03.021.

Bachmair, S., Kohn, I., Stahl, K., 2015. Exploring the link between drought indicators and impacts. Nat. Hazards Earth Syst. Sci. 15 (6), 1381–1397. https://doi.org/10.5194/nhess-15-1381-2015.

Bachmair, S., Svensson, C., Hannaford, J., Barker, L.J., Stahl, K., 2016. A quantitative analysis to objectively appraise drought indicators and model drought impacts. Hydrol. Earth Syst. Sci. 20 (7), 2589–2609. https://doi.org/10.5194/hess-20-2589-2016.

Beguería, S., Vicente-Serrano, S.M., Reig, F., Latorre, B., 2014. Standardized precipitation evapotranspiration index (SPEI) revisited: Parameter fitting, evapotranspiration models, tools, datasets and drought monitoring. Int. J. Climatol. 34 (10), 3001–3023. https://doi.org/10.1002/joc.3887.

Below, R., Grover-Kopec, E., Dilley, M., 2007. Documenting drought-related disasters: a global reassessment. J. Environ. Develop. 16 (3), 328–344. https://doi.org/10.1177/1070496507306222.

Bhalme, H.N., Mooley, D.A., 1980. Large-scale droughts/floods and monsoon circulation. Mon. Weather Rev. 108 (8), 1197–1211. https://doi.org/10.1175/ 1520-0493(1980)108<1197:LSDAMC>2.0.CO;2.

Blauhut, V., Stahl, K., Stagge, J.H., Tallaksen, L.M., Stefano, L. De, Vogt, J., 2016. Estimating drought risk across Europe from reported drought impacts, drought indices, and vulnerability factors. Hydrol. Earth Syst. Sci. 20 (7), 2779–2800. https://doi.org/10.5194/hess-20-2779-2016.

Corzo Perez, G.A., Van Huijgevoort, M.H.J., Voß, F., Van Lanen, H.A.J., 2011. On the spatio-temporal analysis of hydrological droughts from global hydrological models. Hydrol. Earth Syst. Sci. 15 (9), 2963–2978. https://doi.org/10.5194/hess-15-2963-2011.

Guha-Sapir, D. (2018). EM-DAT: The Emergency Events Database - Université catholique de Louvain (UCL) - CRED. Retrieved from www.emdat.be

Diaz, V., Corzo, G., Lanen, H. A. J. Van, and Solomatine, D. P. (2019). 4 -Spatiotemporal Drought Analysis at Country Scale Through the Application of the STAND Toolbox. In G. Corzo & E. A. Varouchakis (Eds.), Spatiotemporal Analysis of Extreme Hydrological Events (pp. 77–93). Elsevier. https://doi.org/https://doi.org/10.1016/B978-0-12-811689-0.00004-5

Diaz, V., Corzo Perez, G. A., Van Lanen, H. A. J., and Solomatine, D. (2018). Intelligent drought tracking for its use in Machine Learning: implementation and first results. (G. La Loggia, G. Freni, V. Puleo, & M. De Marchis, Eds.), HIC 2018. 13th International Conference on Hydroinformatics (Vol. 3). Palermo: EasyChair. https://doi.org/10.29007/klgg

Goswami, B.N., Venugopal, V., Sengupta, D., Madhusoodanan, M.S., Xavier, P.K., 2006. Increasing trend of extreme rain events over India in a warming environment. Science 314 (December), 1442–1445. https://doi.org/ 10.1126/science.1132027.

Herrera-Estrada, J.E., Satoh, Y., Sheffield, J., 2017. Spatio-temporal dynamics of global drought. Geophys. Res. Lett. 2254–2263. https://doi.org/10.1002/ 2016GL071768.

Lloyd-Hughes, B., 2012. A spatio-temporal structure-based approach to drought characterisation. Int. J. Climatol. 32 (3), 406–418. https://doi.org/10.1002/joc.2280.

Mailya, G., Mishra, V., Niyogi, D., Tripathi, S., Govindaraju, R.S., 2015. Trends and variability of droughts over the Indian monsoon region. Weather Clim. Extremes 12 (2014), 43–68. https://doi.org/10.1016/j.wace.2016.01.002.

Mckee, T. B., Doesken, N. J., and Kleist, J. (1993). The relationship of drought frequency and duration to time scales. AMS 8th Conference on Applied Climatology, (January), 179–184. https://doi.org/citeulike-article-id:10490403

Mishra, A.K., Singh, V.P., 2010. A review of drought concepts. J. Hydrol. 391 (1–2), 202–216. https://doi.org/10.1016/j.jhydrol.2010.07.012.

Mishra, V., Aadhar, S., Akarsh, A., Pai, S., and Kumar, R. (2016). On the frequency of the 2015 monsoon season drought in the Indo-Gangetic Plain. Geophysical Research Letters, (April). https://doi.org/10.1002/2016GL071407

Naresh Kumar, M., Murthy, C.S., Sesha Sai, M.V.R., Roy, P.S., 2012. Spatiotemporal analysis of meteorological drought variability in the Indian region using standardized precipitation index. Meteorol. Appl. 19 (2), 256–264. https://doi. org/10.1002/met.277.

Sheffield, J., Andreadis, K.M., Wood, E.F., Lettenmaier, D.P., 2009. Global and continental drought in the second half of the twentieth century: Severity-areaduration analysis and temporal variability of large-scale events. J. Clim. 22 (8), 1962–1981. https://doi.org/10.1175/2008JCLI2722.1.

Sheffield, J., and Wood, E. F. (2011). Drought: Past problems and future scenarios. (P. Earthscan, Ed.). London.

- Stagge, J.H., Kohn, I., Tallaksen, L.M., Stahl, K., 2015. Modeling drought impact occurrence based on meteorological drought indices in Europe. J. Hydrol. 530, 37–50. https://doi.org/10.1016/j.jhydrol.2015.09.039.
- Tallaksen, L.M., Hisdal, H., Van Lanen, H.A.J., 2009. Space-time modelling of catchment scale drought characteristics. J. Hydrol. 375 (3–4), 363–372. https://doi.org/10.1016/j.jhydrol.2009.06.032.
- Tallaksen, L. M., and Van Lanen, H. A. J. (2004). Hydrological Drought Processes and Estimation Methods for Streamflow and Groundwater. Developments in Water Sciences 48. (L. M. Tallaksen & H. A. J. Van Lanen, Eds.). The Netherlands: Elsevier B.V.
- Tase, N. (1976). Area-deficit-intensity characteristics of droughts. Colo. State Univ., Fort Collins, Colo., Hydrol. Pap. 87.
- Van Lanen, H.A.J., Wanders, N., Tallaksen, L.M., Van Loon, A.F., 2013. Hydrological drought across the world: Impact of climate and physical catchment structure. Hydrol. Earth Syst. Sci. 17 (5), 1715–1732. https://doi.org/10.5194/hess-17-1715-2013
- Van Loon, A.F., 2015. Hydrological drought explained. Wiley Interdisciplinary Rev.: Water 2 (4), 359–392. https://doi.org/10.1002/wat2.1085.
- Vicente-Serrano, S.M., Beguería, S., López-Moreno, J.I., 2010. A multiscalar drought index sensitive to global warming: The standardized precipitation evapotranspiration index. J. Clim. 23 (7), 1696–1718. https://doi.org/10.1175/ 2009[CLI2909.1.
- Vicente-Serrano, S.M., Beguería, S., Lorenzo-Lacruz, J., Camarero, J.J., López-Moreno, J.I., Azorin-Molina, C., Sanchez-Lorenzo, A., 2012. Performance of drought

- indices for ecological, agricultural, and hydrological applications. Earth Interact 16 (10). https://doi.org/10.1175/2012EI000434.1.
- Wanders, N., van Lanen, H. A. J., and van Loon, A. F. (2010). Indicators for Drought Characterization on a Global Scale. WATCH Technical Report No. 24. Retrieved from http://www.eu-watch.org/media/default.aspx/emma/org/10646416/WATCH+Technical+Report+Number+24+Indicators+For+Drought +Characterization+on+a+Global+Scale.pdf
- Wilhite, D. A. (Ed). (2000). Drought as a natural hazard: concepts and definitions. In DROUGHT, A Global Assessment, Vol I and II, Routledge Hazards and Disasters Series. Routledge, London.
- World Meteorologic Organization (WMO). (2012). Standardized Precipitation Index user guide. WMO-No. 1090. Geneva, Switzerland. Retrieved from http://library.wmo.int/pmb_ged/wmo_1090_en.pdf
- Xu, K., Yang, D., Yang, H., Li, Z., Qin, Y., Shen, Y., 2015. Spatio-temporal variation of drought in China during 1961–2012: A climatic perspective. J. Hydrol. 526, 253– 264. https://doi.org/10.1016/j.jhydrol.2014.09.047.
- Yevjevich, V., 1967. An objective approach to definitions and investigations of continental hydrologic droughts. Hydrology Paper 23 Retrieved from Fort Collins, Colorado. Vol, 23).
- Yevjevich, V., and Karplus, A. K. (1973). Area-time structure of the monthly precipitation process. Colo. State Univ., Fort Collins, Colo., Hydrol. Pap. 64.
- Zaidman, M.D., Rees, H.G., Young, A.R., 2002. Spatio-temporal development of streamflow droughts in north-west Europe. Hydrol. Earth Syst. Sci. 6 (4), 733– 751. https://doi.org/10.5194/hess-6-733-2002.